NASA CR-159777

(NASA-CR-159777) MONODISPERSE ATOMIZERS FOR AGRICULTURAL AVIATION APPLICATIONS Final Report (FWG Associates, Inc.) 81 p HC A05/MF A01 CSCL 20D

N80-19450

Unclas G3/34 47415

MONODISPERSE ATOMIZERS FOR AGRICULTURAL AVIATION APPLICATIONS

Larry S. Christensen and Sidney L. Steely

FWG Associates, Inc.
R.R. 2, Box 271-A
Tullahoma, Tennessee 37388

Prepared for

NATIONAL AERONAUTICS AND SPACE ADMINISTRATION
Lewis Research Center
Cleveland, Ohio 44135

February 1980

Contract NAS3-21582

TABLE OF CONTENTS

SECTION—— PAGE

1.0 INTRODUCTION

The question of whether a pesticide will perform its intended function without unreasonable adverse effects on the environment has been a searching question since the first pesticides were applied. Today the predominant formulations used for pesticide applications on plant foliage are sprays. The majority of spray nozzles used produce a wide range of spray droplet diameters. These droplet size distributions strongly influence the degree to which the released chemical deposits on the intended target swath area. Generally, the amounts of chemical that cause obvious damage are the result of swath overlapping onto a nearby susceptible crop. However, small spots or leaf burn, especially if the leafy crop is an edible product, can occur with actual deposited residues of less than 0.03 ppm of chemical in plant tissue. This damage is usually caused by the small droplets. Spray droplet sizes of less than 50 microns diameter are easily transported by meteorological conditions and possible damage to susceptible crops occurs. Unfortunately, the majority of spray nozzles produce a wide range of spray droplet diameters, including a great number of small droplets. If the droplet size distribution is monodisperse, however, the prediction of swath coverage and elimination of drift is greatly facilitated. Droplets of similar size will typically all drift equivalent distances and consequently deposit at the same position.

The purpose of this research is to conceptually develop two nozzle designs which will produce monodisperse droplets for agricultural purposes over the range of fluid physical characteristics of pesticide formulations and for droplet sizes ranging from 25 to 500 μm diameter. The ultimate development of such devices will greatly reduce any adverse effects on the environment due to pesticide application.

Considerable research has been conducted on the theory and performance of atomization equipment in several professional areas, including physics, mathematics, mechanical engineering, chemical

engineering, and agricultural engineering. These areas of endeavor were thoroughly investigated in order to utilize previously obtained information in regard to monodisperse droplet production.

The present work consists of a thorough literature search concerned with monodisperse droplet production and the range of physical characteristics of pesticide formulations. Searches of the open literature and computer g: ernment agency searches were conducted. Many universities and agriculture research facilities were visited in an attempt to obtain the most recent information concerning nozzle development and pesticide formulation physical characteristics. Two new conceptual ideas were then determined and the effectiveness of each technique over the range of physical fluid characteristics encountered in pesticide formulations were assessed. The different techniques of producing monodisperse droplets were assessed and rated as to their potential for practical application of pesticide formulations. The information obtained during the present project should be beneficial in other areas where droplet production plays a significant role in the overall research objectives. The material reported herein can effectively be used as a base for further development of monodisperse droplet generators for agricultural applications.

A brief review of monodisperse atomization techniques is presented in Section 2.0 of this report. Section 3.0 contains a synopsis of the information obtained concerning agricultural aviation spray applications. The conceptual ideas, designs and rationale are presented in Section 4.0. Concluding remarks and recommendations are given in Section 5.0, while references are given in Section 6.0.

2.0 DROPLET PRODUCTION TECHNIQUES

A brief presentation of the different types of monodisperse droplet production techniques are given in this section. Pertinent information, such as mean drop diameter and drop distribution uniformity is presented. The potential of each technique for applicability to agricultural aviation spraying is rated. For easy comparison of the different techniques the following rating system has been developed. The techniques are rated from one to five, one indicating very little potential, two to three indicating the technique shows some potential, and four to five indicating the technique shows good potential for agricultural aviation spraying operations. The rating given to each of the techniques is presented in each subsection and a summary of the results presented at the end of this section.

The rating of each technique was based on a number of weighting factors. The following factors were used: monodispersity, droplet sizes which can be produced, application rates, practicality, simplicity, and economic viability and assigned the following weights (percentage):

1.	Monodispersity	30%
2.	Droplet Sizes Which Can Be Produced	25%
3.	Application Rates	15%
4.	Practicality	15%
5.	Simplicity	10%
6.	Economic Viability	5%

Monodisperse sprays shall be defined as having three characteristic drop diameters: D_{av}, D_{max}, and D_{min}, respectively. They are defined as follows:

$D_{av} = 1/2(D_{max} + D_{min})$

$D_{max} \leq 1.2\ D_{av}$, where 95 percent of the drops on a weight basis are smaller than D_{max}

$D_{min} \geq 0.8\ D_{av}$, where 5 percent of the drops on a weight basis are smaller than D_{min}.

The monodispersity and droplet size range most significantly effect the efficacy of a spray dispersal system and therefore were weighted most heavily. There exists an optimum drop size for each agricultural application which depends on such things as target size and shape and meteorological conditions. By effectively controlling the droplet size the optimum amount of chemical can be applied with the least amount of capital spent and with a minimum of degradation to the environment. Monodispersity, assuming homogeneous mixing, will also help to insure that each drop contains approximately the same amount of active ingredient and behaves similarly aerodynamically. Drift of small droplets with possible subsequent damage and ineffective overcoverage with large droplets can be largely eliminated. Use of a monodisperse droplet distribution will, therefore, greatly help to overcome some of the major problems confronting aerial application today. Application rates and practicality were rated as moderately important at this stage of the new conceptual nozzle development. Insufficient application could result in the pest not being effectively controlled and therefore the application rate and/or solution concentrations must be appropriately altered. Any new instrument developed must have at least the potential for application to aerial operations. It would also be beneficial if the device developed were simple and economically viable. A nozzle which could be used with conventional, already-operating, peripheral equipment would be an excellent addition to present spray technology. Technique ratings and descriptions are presented below.

2.1 An Apparatus for the Production of Uniform-Sized Water Drops at Desired Time Intervals with Diameters between 0.4 and 2.0 mm

Many experimental studies require the use of water drops of uniform size produced at controlled time intervals. In order to accomplish this, some devices employ a vibrating system which modulates a jet in the direction of its motion, or breaks the jet at right angles to its direction of motion. Similar devices for producing uniform drops by a

continuous airflow have also been developed [1]. With these vibrating, jet-type, droplet generators, water flows through a fine capillary and a drop forms at the capillary tip. A continuous airflow concentric with the tip blows the drop off as it reaches a particular size, this size is determined by the air velocity, the flow rate through the capillary, and the orifice diameter.

2.1.1 Construction and Operation

The device described in this subsection is a modified version of the above system, designed so that the airflow is intermittent and has a minimum influence on the drop subsequent to its release. Figure 2.1 gives a schematic of the apparatus. The water first passes through a primary filter to remove particles down to 0.5 μm and then through an ionic exchange column. The water is then fed to a variable height reservoir, open to the atmosphere, via a 0.1 μm millipore filter. Water flows from this reservoir through a second 0.1 μm millipore filter, whose primary purpose is to provide resistance to the flow. The drop-producing head consists of four pieces of stainless steel hypodermic tubing, gauged and telescoped from largest to smallest size and silver soldered at the joints. The largest diameter needle serves both to increase the rigidity of the system and to inhibit any oscillation tendencies. As water flows through the capillary, drops form on its end and are blown off by an air pulse concentric with the tip. This air pulse is produced by opening a solenoid valve for a time of 0.01 second. A timing circuit enables pulses to be applied at intervals down to about one-quarter second to an accuracy of at least one part in 10^3. Air is supplied via a reducing valve at pressures varying from 0.2 to 1.0 atmospheres for the largest and smallest drops, respectively. The drop-producing head is supported in a glass tube 25 mm diameter with four centering screws. This tapers to a tube 5 mm diameter containing seven stainless steel tubes surrounding the capillary which serve to smooth the airflow. Drops can be produced at a required interval and having a required diameter by varying the flow rate of the water and the pulse rate of the solenoids. The upper limit of drop size is delineated by the drop which is just large enough to fall from the needle under gravity

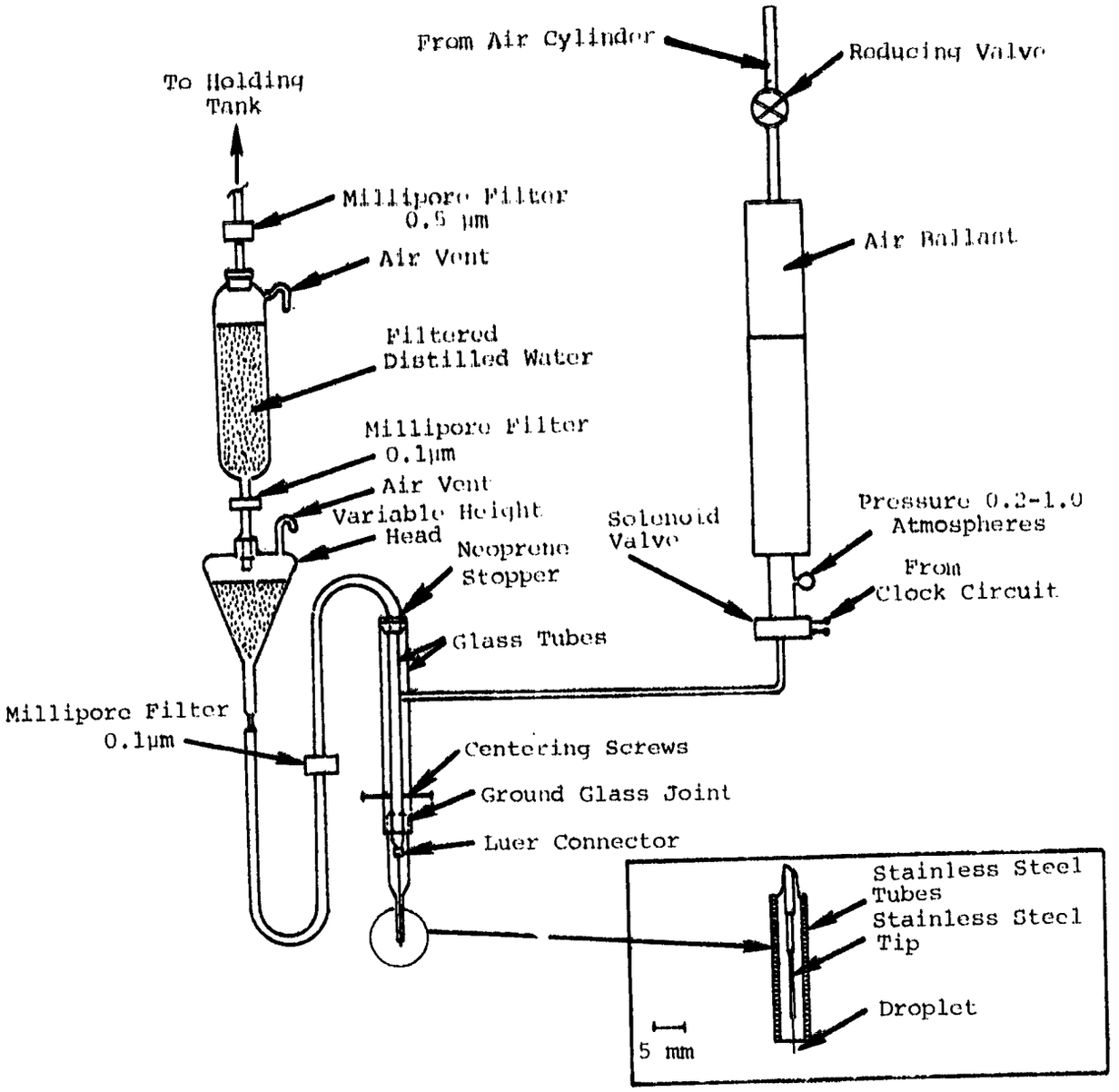

Figure 2.1 Apparatus used for the production of uniform size drops (0.4 to 2.0 mm diameter).

(> 2.0 mm). The lower limit is delineated by the smallest size of capillary which can be accurately machined and by irregularities in the air pulse (~ 0.4 mm). At times, a rough needle tip or clogging of the nozzle by particles which bypass the filtration system or deposit from the outside air cause the smaller droplets to be blown off with some sideways momentum. It is probably practical to reduce clogging from outside contaminants by allowing the water to flow continuously through the tip of the capillary over the entire period of its use. The drops are observed to oscillate after they have detached from the tip. An illustration of droplet formation and oscillation is presented in Figure 2.2. The subsequent droplet trajectories depend on whether or not these oscillations die out or are reinforced by eddy shedding as the drop approaches its terminal velocity.

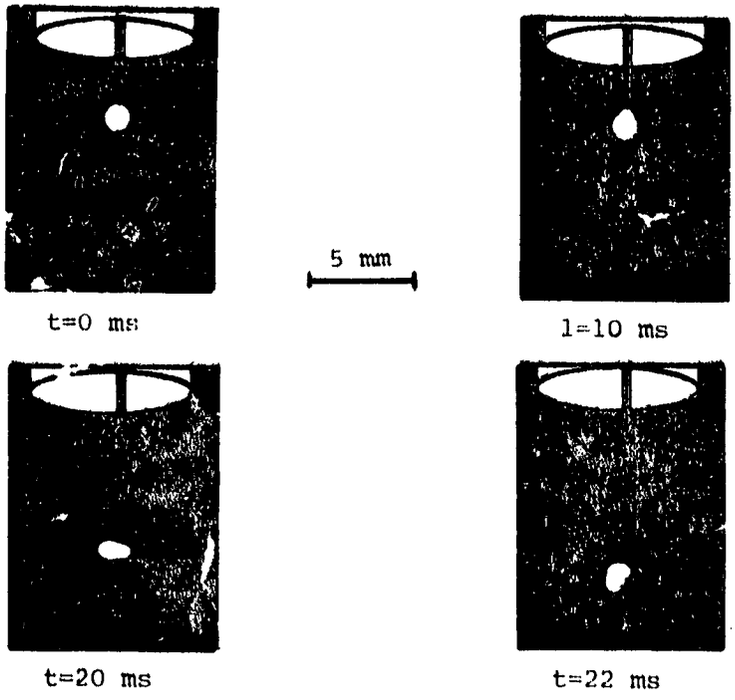

Figure 2.2 Sequential photographs of a drop 1.0 mm in diameter being produced from a needle tip by an air pulse.

2.1.2 Drop Distributions and Rating

The variation and size of successive drops were determined by collecting drops under silicone fluid with a viscosity of approximately 10^4 centistokes and measuring their diameter with a calibrated microscope stage. Previous investigations [2] have shown that the major variation in droplet diameter lies within the microscope measurement limits, giving standard deviations of 1.5 percent for 0.45 mm diameter drops and 0.5 percent for 1.8 mm diameter drops. The results are illustrated in Figure 2.3, where d is the droplet diameter and d_m is the mean droplet diameter. The graph indicates that the technique is capable of producing droplets within the definition of "monodisperse."

In rating this technique as to its potential for use in agricultural spray applications, one must first consider the drop size range which this device is able to produce. The drop size range is from 0.4 mm to 2.0 mm and therefore does not encompass the drop size range desired (25 to 500 μm). This particular method of drop production does indeed produce droplets of uniform size; however, the droplet production rate is much lower than that required for agrigultural applications. On a rating scale of one to five, five being the highest (greatest potential for agricultural applications), this particular method of drop production is assigned a rating of 1.30. The method, however, does show promise for production of droplets in the intermediate size range, i.e., those droplets approximately 1 mm which are not usually produced by vibrating devices or hypodermic needles The generator can therefore be an effective tool in the laboratory for studying interactions between droplets of approximately 1 mm diameter.

2.2 The Production of "Monodisperse" Water Droplets from 2 to 500 μm Diameter

The method to be described here is used for the production of "monodisperse" water droplets between 2 and 500 μm diameter and uses the fact that when bubbles of a given size burst at an air/water interface, the collapse of the bubble cavity produces an upward moving jet (Rayleigh jet) which quickly disintegrates into several small drops. Each of

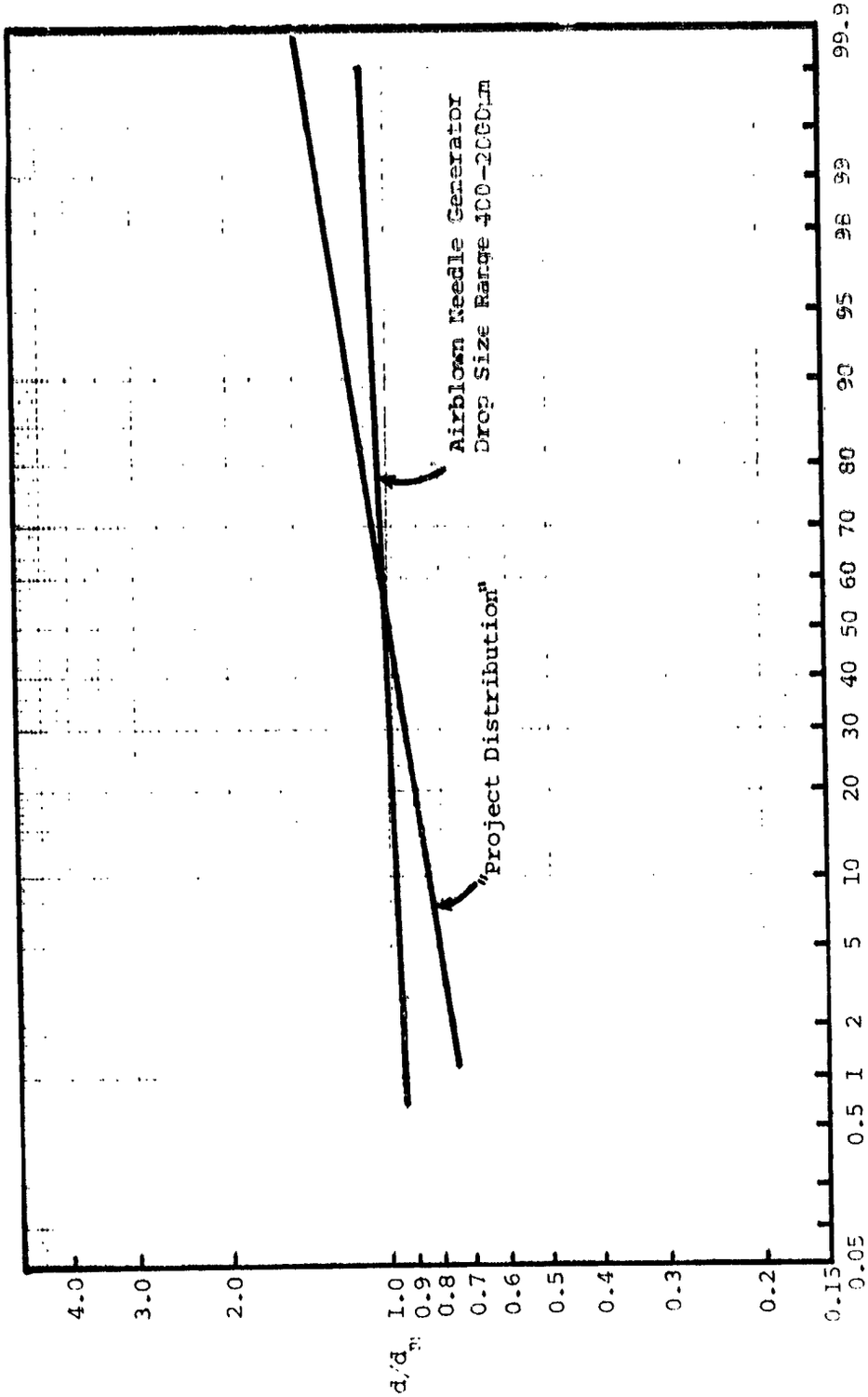

Figure 2.3 Drop size distributions--needle air generator.

these drops, not necessarily of equal diameter, rises to a height which is remarkably constant from one bubble to the next. The droplets, which correspond to each of these rise heights, have nearly equal diameters [3].

The experimental setup requires simply a stream of bubbles rising in a water container. Previous high-speed photographs have shown conclusively that upon collapse of a bubble a narrow jet rises rapidly from the bubble cavity [3], and within a distance of one bubble diameter the jet proceeds to breakup into five or six droplets, all of which rise to characteristic heights. With a consistent bubble size, these heights are systematically obtained, thus indicating the reproducibility of the various droplet diameters at different rise heights.

2.2.1 Experimental Methods

The production of a steady stream of uniform bubbles of any diameter is easily accomplished (greater than 50 μm) by forcing air through fine tips produced by drawing out a length of glass capillary tubing. The size of the bubble is a function of the bore diameter.

If the bubbles are allowed to rise in distilled water, they will break immediately on contact with the clean surface. It is sometimes necessary to have the glass capillary tip near the surface to prevent the coalescence of bubbles as they rise through the water. As each bubble breaks, an upward-moving, high-velocity jet will form and break into a series of droplets. These droplets rise at speeds of several hundreds of centimeters per second. The frictional retarding force at such high speeds causes a rapid deceleration and loss of kinetic energy. For a given bubble diameter, each of the drops will rise to a height which is remarkably reproducible.

With small bubbles and a high rate of production, one is able to produce drops at such a rate that 30 or more of the drops are airborne simultaneously. The droplet fall velocities can be obtained by measuring the vertical component of photographic streaks which represent the drop's motion during a photographic exposure, and dividing by the exposure time. Using the fall velocities of the different drops, the droplet diameters were determined.

2.2.2 Drop Size Distributions and Rating

This particular method of producing "monodisperse" droplets is well-suited for a laboratory environment. Figure 2.4 illustrates the type of droplet distributions which can be obtained. The droplet size covers the range from 2 to 500 μm. However, the production rate is very low and is not compatible with application rates for agricultural aviation applications. The technique involves selecting one droplet from a jet then propelling the droplet to a region outside the aircraft boom. This is a complicated engineering problem. This problem, together with other features, such as surface characteristics, bubble production, and coalescence render this technique impractical for agricultural aviation applications. The technique most likely can be used effectively in a laboratory environment for production of monodisperse drops in the 2 to 500 μm range. Using the rating system previously described, this droplet production method is assigned a rating of 1.15.

2.3 Vibrating Capillary Devices for Production of Uniform Water Droplets

The first droplet generators of this type were produced to study the collision and coalescence of small water droplets. Vibrating capillary devices consist of a hypodermic needle vibrating at its resonant frequency and can produce uniform streams of droplets down to 30 μm diameter. The size and frequency with which the droplets can be produced depends upon the flow rate of the liquid through the needle, the needle diameter, the resonant frequency, and the amplitude of oscillation of the needle tip. Drops can be produced from 30 to 1000 μm diameter.

2.3.1 Construction and Operation

A schematic of the droplet generator is shown in Figure 2.5. The droplet generator shown in Figure 2.5 was produced by Mason, et al. [4]. A stainless steel, hypodermic needle, N, through which the water from the reservoir, R, is forced at a constant rate, fits snugly into a small central hole in a cylindrical spigot, S, which is cemented to the center of an iron diaphragm, D, of an electromagnetically driven earphone. The energizing coil, C, of an electromagnet, M, is connected to an audiofrequency

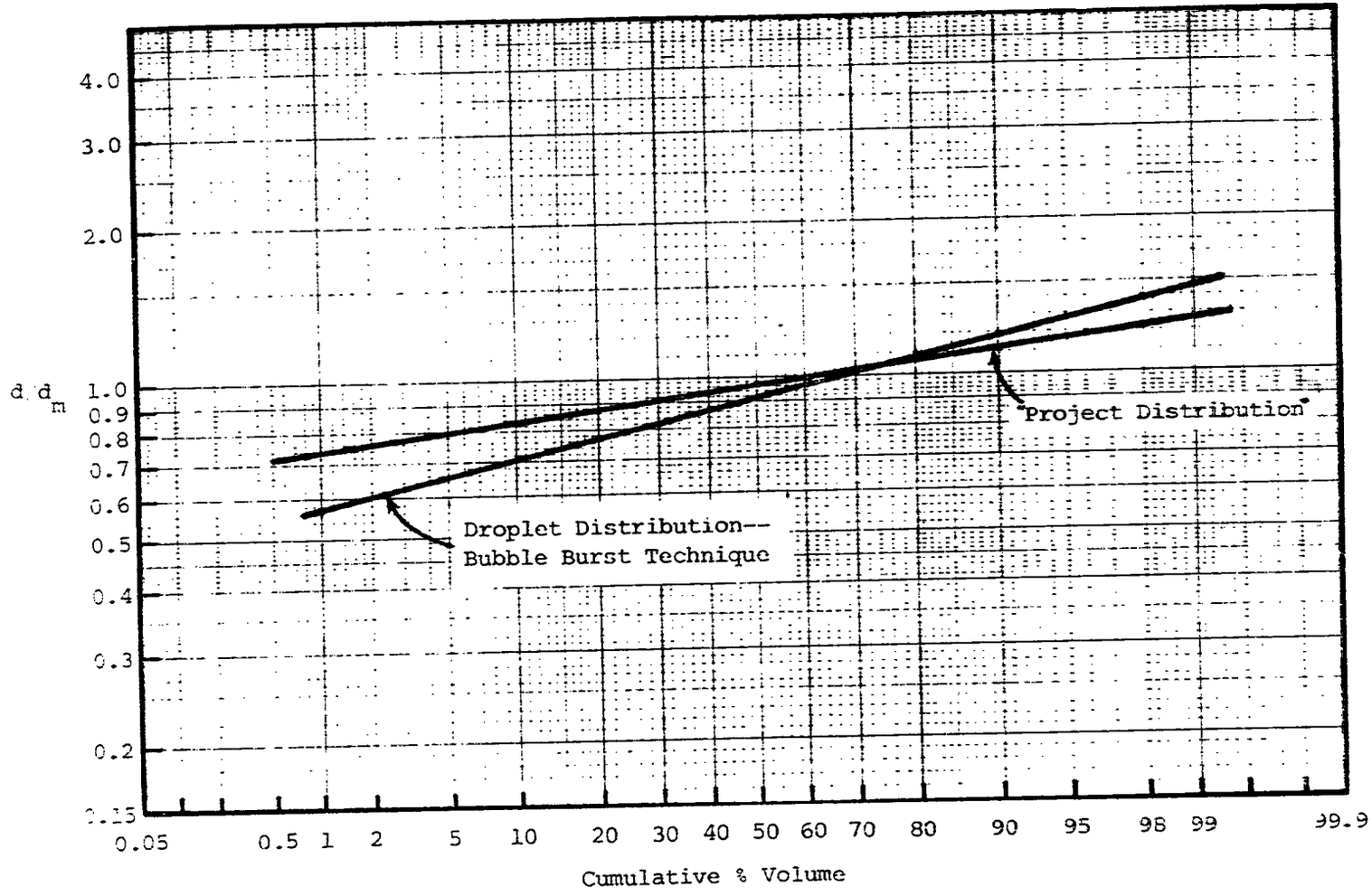

Figure 2.4 Drop size distribution--bubble burst technique.

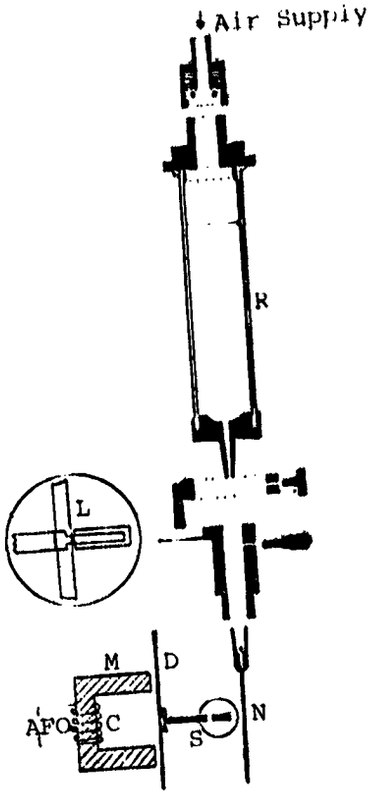

Figure 2.5 Schematic of a vibrating capillary device [4].

oscillator and causes the needle to vibrate mechanically by the movement of the diaphragm and spigot. The frequency of the oscillator is varied until the tip of the needle vibrates in a resonant mode with an amplitude of several millimeters. The resonance frequency, which is determined not only by the characteristics of the needle but also by the masses and dimensions of the diaphragm and spigot. The frequency range at which resonance occurs is relatively small.

The stability of the droplet stream is particularly dependent upon the flow rate of the liquid and it is essential to keep the flow rate constant. To accomplish this, water can be forced from the reservoir using compressed air rather than a large constant head to maintain monodisperse droplet distributions. One must also insure that the needle vibrates in the same stable mode for long periods of time. To accomplish this it is necessary to prevent the needle from moving in the

spigot, and this is achieved by a small locking device, L, shown in Figure 2.5. Observations [4] of the needle tip, have revealed that for a given needle and amplitude of vibration, a critical volume of liquid must accumulate before it can be flung off by a change in direction of the needle. Figure 2.6 shows a stream of droplets produced from a thread of liquid issuing from a tip of a hypodermic needle. At low flow rates, the needle may execute several oscillations before the critical volume is reached and there is a tendency for the liquid to be ejected as a single drop. As the flow rate is increased, a single drop may be ejected at each turning point of the needle and finally at high flow rates, the issuing liquid is drawn out into a thread by the receding tip and usually breaks up into a series of progressively smaller masses. For a constant orifice diameter, the length of the thread increases with increasing pressure head. Different diameter drop sizes are projected in different directions. The number of streams may be controlled by the frequency and vibration amplitude.

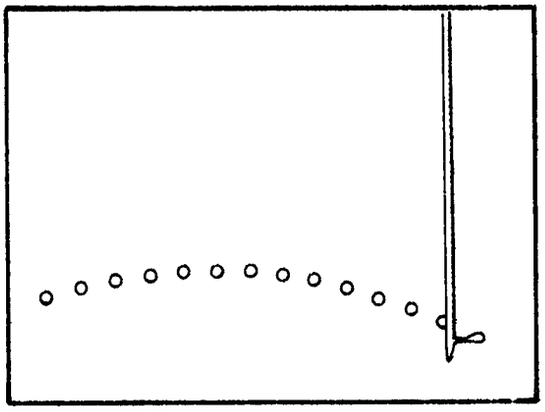

Figure 2.6 Stream of droplets produced from a thread of liquid issuing from the tip of a hypodermic needle.

2.3.2 Drop Size Distribution and Rating

A standard 30 gauge hypodermic needle (bore diameter 140 μm) can produce drops of radius 80 to 200 μm at frequencies of about 300 Hz. By adjusting the amplitude of vibration and the liquid flow rate it is possible to obtain a single stable droplet stream of any desired radius

between 140 and 200 μm. To produce even smaller droplets the needle can be rebored to produce stable streams of droplets 30 μm diameter at resonant frequencies of between 500 and 1000 Hz. Droplet diameters of greater than 400 μm are readily produced with needles of larger gauge. The type of drop size distributions which can be obtained using this droplet production method are shown in Figure 2.7.

The vibrating capillary generator is a very effective device for producing small individual monodisperse droplets. The device is usually used in a laboratory environment. The potential of such a system being effectively utilized for agriculture applications is not the best. The number of droplets produced is severely limited and nozzle clogging could be a serious problem. The drop size range covers, however, the range of droplets desired. This technique is assigned a rating of 2.40.

2.4 Ultrasonic Nebulizers

There are a number of commercially available nebulizers and atomizers which employ ultrasonic vibrations to atomize bulk liquid. Ultrasonic nebulizers are capable of producing high aerosol concentrations and are widely used in aerosol medical therapy.

2.4.1 The Process of Nebulization

In ultrasonic nebulizers, the mechanical energy necessary to atomize the liquid comes from a piezoelectric crystal vibrating under the influence of an alternating electric field produced by an electronic high frequency oscillator. The vibrations are transmitted through a coupling liquid to a nebulizer cup containing the solution to be aerosolized. At low intensities, capillary waves are formed at the air/liquid interface. As the intensity increases, a fountain of liquid surrounded by a heavy mist appears at the center of the cup. The mean size of the droplets making up the mist is related to the wavelength of the capillary waves which decreases with increasing frequency of the ultrasonic vibrations. Once formed, the droplets are immediately subjected to a number of influences tending to alter their size and dispersity. Because of the increased vapor pressure at the droplet surface, due to curvature, the

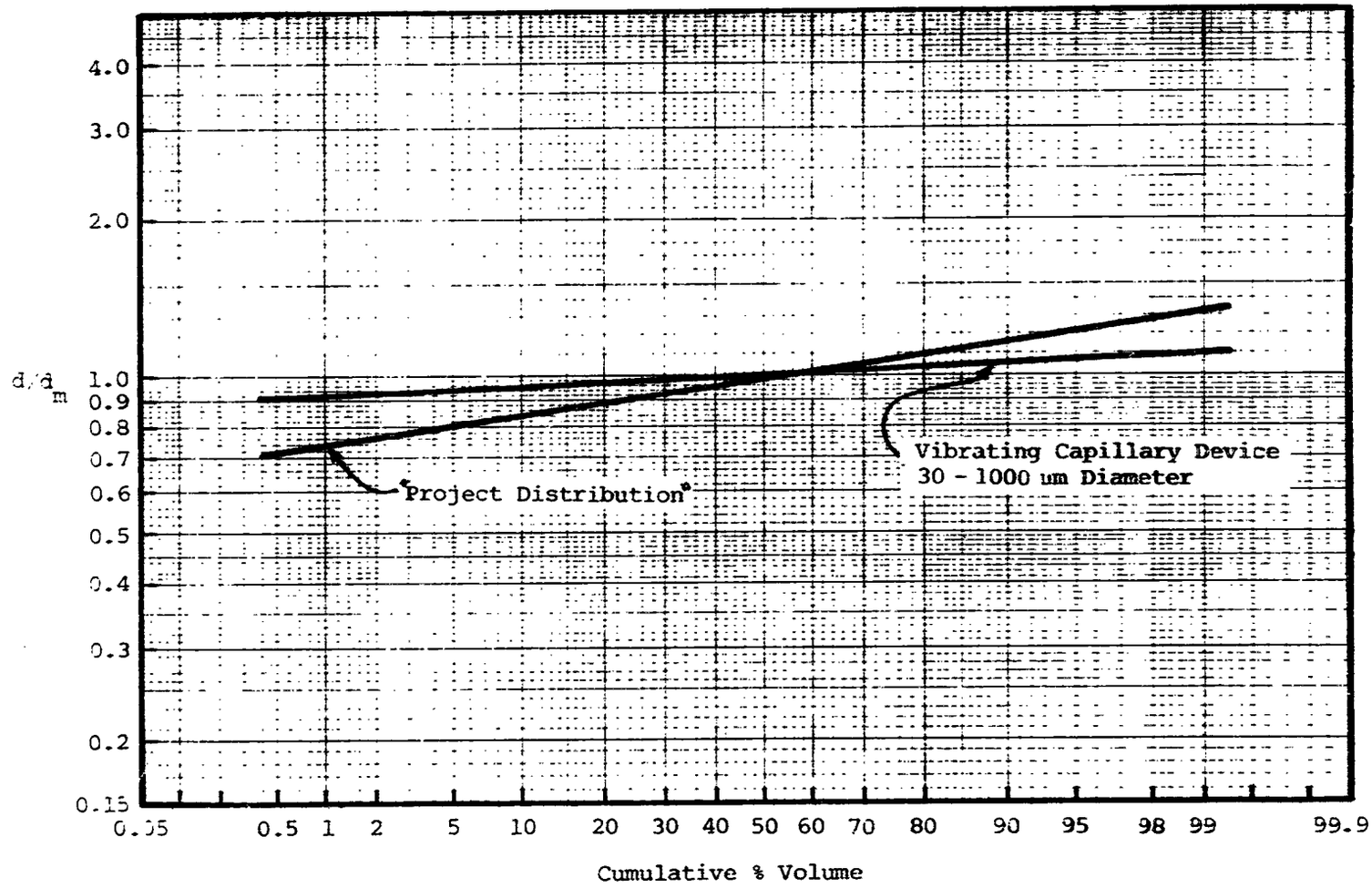

Figure 2.7 Drop size distributions--vibrating capillary device.

drops will undergo some evaporation even in an atmosphere saturated with respect to a flat liquid surface. The large number of droplets per unit volume also favors rapid coalescence. If there is no circulation through the nebulizer, the droplets will coalesce and settle back into the cup. On the other hand, if air is blown through the nebulizer some of the droplets are carried out to form a useful aerosol.

Only a small fraction of the energy introduced into the nebulizer goes into the formation of new surface area necessary to produce droplets; most of it is converted to thermal energy, heating the nebulizer until a temperature is reached at which the input energy just balances the energy carried away by evaporating molecules and by conduction to the surroundings and to air passing through the nebulizer. The water vapor necessary to saturate the air comes partly from the surface of the bulk liquid, including the fountain, and partly from the droplets themselves. When formed, the droplets are at a temperature of the bulk liquid, but cool somewhat due to evaporation. As the droplet-laden, saturated air moves out of the nebulizer into cooler regions, water vapor condenses on the surrounding walls, is partially replaced by additional evaporation of the droplets and, in effect, a transfer of water from the droplets to the walls occurs.

If the bulk liquid is a solution, the evaporation of water from it causes a continual increase in solute concentration. When a reservoir, external to the nebulizer, is used to maintain a constant level of nebulizer solution, the concentration of the latter increases to a equilibrium value depending on the rate at which aerosol and water vapor are carried away.

Several methods of establishing the aerosol output of this type of generator can be used. One of these which allows simultaneous determinations of both aerosol and water vapor contents is based on the following derivation. Let A equal the milliliters of solution per minute leaving the nebulizer as aerosol, W equal the milliliters of water evaporated from the bulk liquid per minute, C_0 equal the initial concentration in the cup and equal to the concentration in the reservoir, C equal the concentration in the cup at time, t, and V equal the volume

of solution in the cup. If both A and W are assumed to be constant with time, then the rate of change of concentration is

$$DC/Dt = -\frac{A}{V}C + \frac{A + W}{V}C_0$$

When integrated, this gives $C = C_0[1 + W/A(1 - e^{-At/V})]$ for large values of At/V, this becomes $C = C_0(1 + W/A)$. During t minutes of operation, the reservoir volume diminishes by an amount $\Delta V = (A + W)t$. Thus by measuring the concentration of the solution in the cup and the volume in the reservoir before and after a given experiment, it is possible to calculate both A and W with the aid of the above equations. Another method of establishing the aerosol output consists of determining the concentration of aerosol in the air passing through the nebulizer, either by collecting all of the aerosol in a known fraction of the nebulizer or by collecting the total aerosol output in an electrostatic precipitator. This method, however, does not permit a determination of the excess vapor lost from the solution.

2.4.2 Droplet Size Distributions and Rating

The output characteristics of this type of generator have been obtained [5]. A diagram illustrating a typical cumulative volume distribution for an ultrasonic nebulizer is given in Figure 2.8. For frequencies below approximately 2 megahertz, the diameters of the drops produced by ultrasonic nebulizers have been shown to be related to the wavelength of the capillary waves produced on the surface of the liquid. Lange [6] found that the count median diameter (C.M.D.) of the droplet size distribution (half of the particles have diameters smaller than the count median diameter) was given by

$$C.M.D. = 0.34(8\pi\sigma/\rho f^2)^{1/3}$$

where σ is the surface tension and ρ is the density of liquid being nebulized, and f is the frequency of the exciting motion. The count median diameter is in μm if σ is in dynes/cm, ρ is in grams/cm^3, and f is in megahertz. Experimental results suggest that coalescence and sedimentation of droplets within the nebulizer have only a negligible effect on the size distribution when there is a continuous, rapid flow

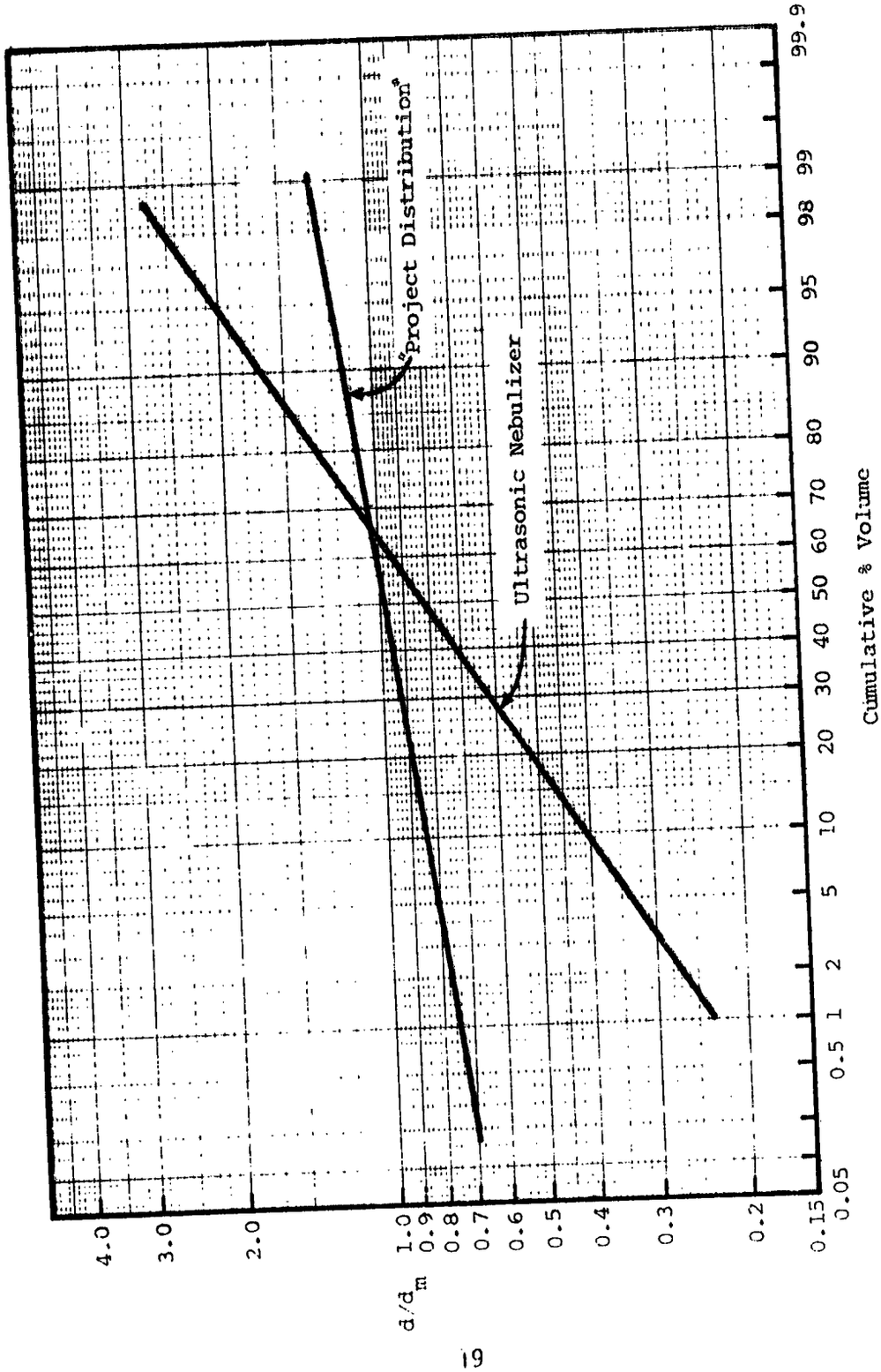

Figure 2.8 Drop size distribution--ultrasonic nebulizer.

of air through the nebulization chamber. However, when there is no flow through the chamber there is a noticeable effect on the size distribution. Drop size distributions obtained using the ultrasonic nebulizers have been tabulated [7]. Initial drop size distributions have mass median diameters of approximately 5.7 to 11.5 μm.

This particular methed of droplet production produces many very small size droplets; however, the volume mean diameter of these droplets is much smaller than that normally used for agricultrual spray applications and droplets in this size range will be very susceptible to drift. This particular method is given a rating of 1.80. With future research in surface characteristics, surface breakup and capillary disruption, this method might be effectively used in agriculture.

2.5 Rotary Atomization

2.5.1 Droplet Production

Droplet production consists of centrifugally accelerating a liquid to a high velocity and discharging it into the atmosphere. The liquid attains its velocity without high pressures. One other attractive aspect of rotary atomization is that the feed rate can be independently controlled.

It now appears that there are three different droplet production mechanisms active when one uses rotary atomizers; namely (1) direct droplet formation, (2) ligament formation, and (3) film formation. In rotary atomization by direct droplet formation, the drops first appear as bulges on the periphery and are then blown off singly. With increased feed rates, these bulges form ligaments which become unstable and eventually break up at some distance from the periphery. At still larger feed rates, the ligaments join to form a continuous film extending a distance out from the periphery before breaking up irregularly into ligaments and large droplets.

In order to obtain uniform droplet distributions from rotary atomizers, it has been suggested [8] that the following conditions be met: (1) disk surfaces should be smooth, (2) the centrifugal force should be

large compared with the gravitational force, (3) disk rotation should be vibrationless, and (4) liquid feed rates should be uniform.

A high degree of drop uniformity was found [8, 9] at low uniform feed rates and when the atomizer was completely wetted. Ligaments and films were not present. When ligaments are present, two principal particle size ranges are sometimes observed. The smaller size range probably consisting of satellite droplets created during the collapse of the ligaments.

Rotary atomization has been summarized in Reference [10]. The drop size distribution from rotary atomizers apparently depends on rotational speed or centrifugal force and the magnitude of the feed rate. At low feed rates and low speeds, mass forces predominate and the droplet size is primarily an inverse function of centrifugal force, at high feed rates and/or high speeds, the drop size is principally an inverse function of peripheral speed. Liquid properties, such as viscosity, surface tension, and density probably influence the range in which the centrifugal force and peripheral speed predominate. Such liquid properties will alsc influence the instability of the ligaments and the subsequent drop formation and size distribution. The rotary atomization technique appears from previous analyses by many different investigators to be particularly suited to fluids with high viscosity.

In order to obtain a monodisperse droplet distribution, one needs to maintain feed rates and peripheral speeds such that droplet production is either by direct droplet formation or ligament formation. A combination of feed rates and peripheral speeds which produce both direct droplet formation and ligament droplet formation will result in a polydisperse droplet distribution.

2.5.2 General Characteristics and Drop Size Distributions of Rotary Atomizers

The rotary atomizer is characterized by the liquid being continuously accelerated by the centrifugal force imparted by the rotating disk, and the liquid is discharged at high radial and peripheral velocities. In contrast, a hydraulic, swirl-type, pressure nozzle obtains its velocity by the conversion of hydraulic pressure to kinetic energy.

There have been a number of studies [10] of various types of rotary devices. Rotary devices, such as vane, smooth, and others have been investigated. No significant variation in the drop size distributions have been detected for atomization at one feed rate and one peripheral velocity. The drop size distributions [10] are plotted in Figure 2.9. The effects of feed rate and disk speed on drop size distribution from vane disk atomizers have been studied [11]. The results are shown in Figures 2.10 and 2.11. Several mechanisms for production of the droplets have been expounded. First, that direct drop formation can be controlled by centrifugal force, while atomization by ligament and film formation might be controlled by peripheral speed. It can be noted that none of the drop size distributions obtained fit within the distribution criteria as set forth as project objectives; however, this does not entirely preclude the conceptual idea of rotary atomization as a viable technique for production of monodisperse droplets for agricultural purposes.

Recently, further investigations into the production of monodisperse droplets using rotary atomizers have been carried out [12]. The physical performance of the rotary atomizer was examined including the motor characteristics, the feed rates, and the drop size spectra. Experimental studies were carried out using an oil because of its low volatility. The droplets were sampled in a settling chamber. Three MgO coated slides were placed on upturned petri dishes on the floor of the chamber, one at the center and one on either side along the line bisecting the open side of the chamber. Droplet distributions were obtained over a range of rotating speeds using different restriction washers. A graph showing the droplet diameter as a function of rotation speed in revolutions per minute is shown in Figure 2.12. Table 2.1 contains an overall synopsis of the information obtained. Figures 2.13 and 2.14 illustrate the type of droplet distributions which can be obtained. The distributions are much more uniform than those obtained using hydraulic pressure or liquid atomizing techniques.

The experimental information obtained indicates that droplet size varies with flow rate as well as rotational speed. At a given rotation

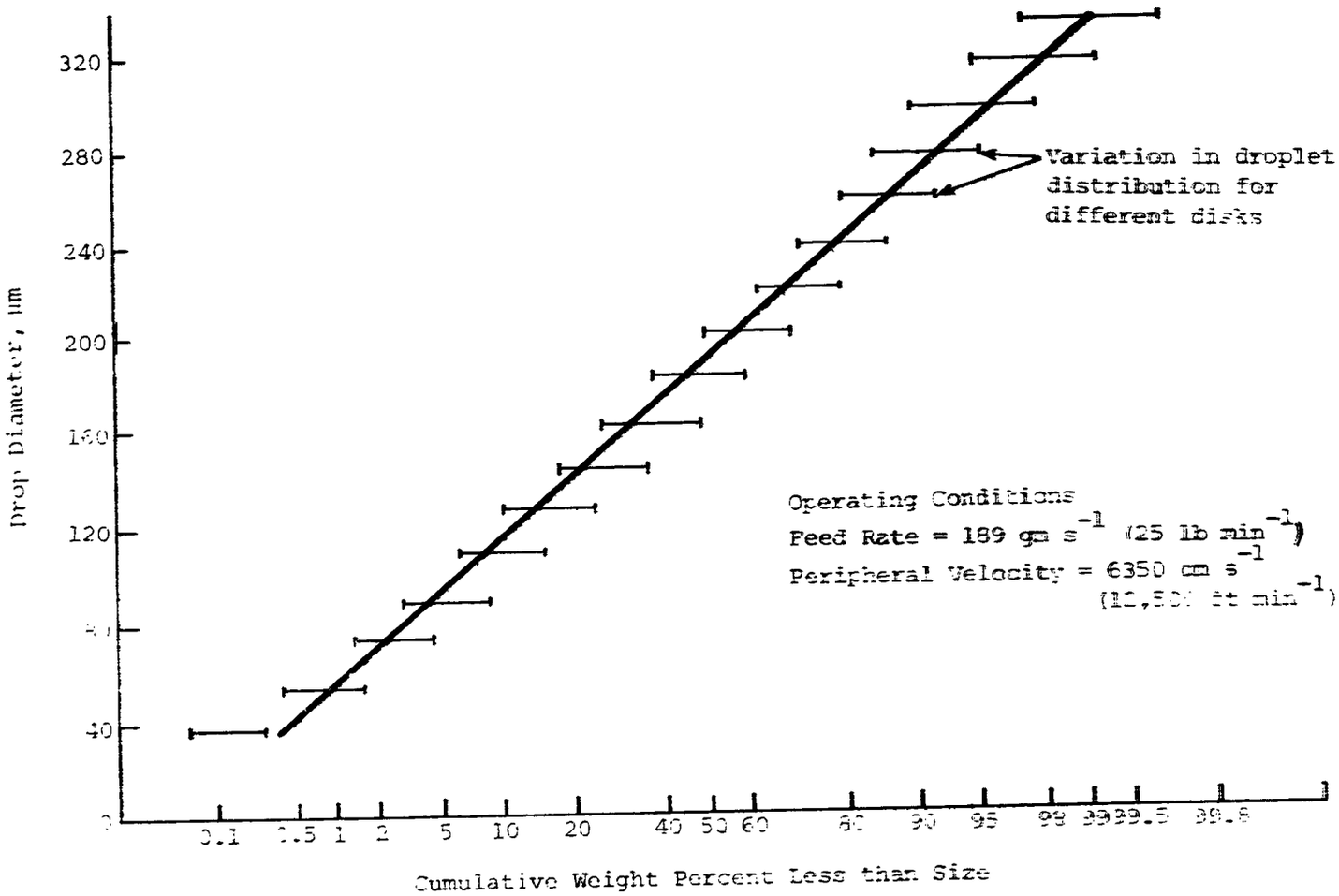

Figure 2.9 Variation in drop size distribution from various disk atomizers [10].

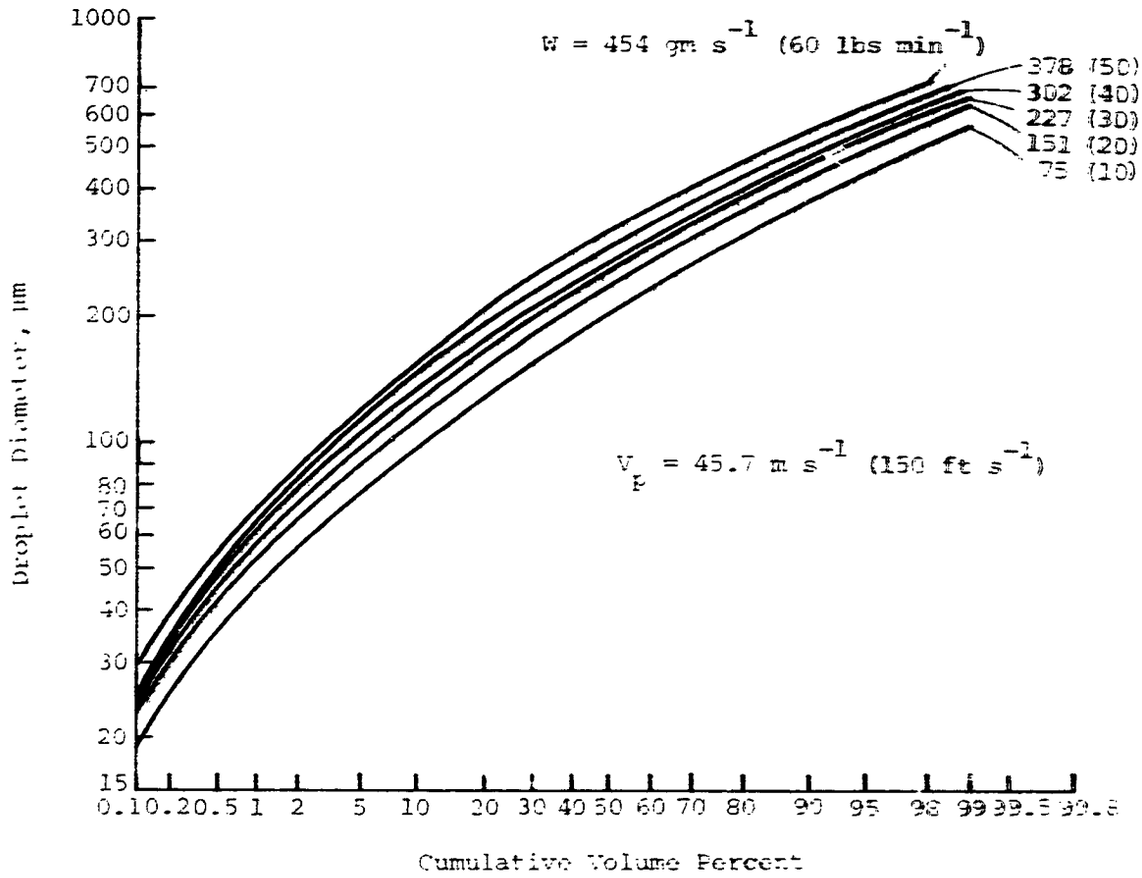

Figure 2.10 Drop size distributions from vaned disks for various feed rates.

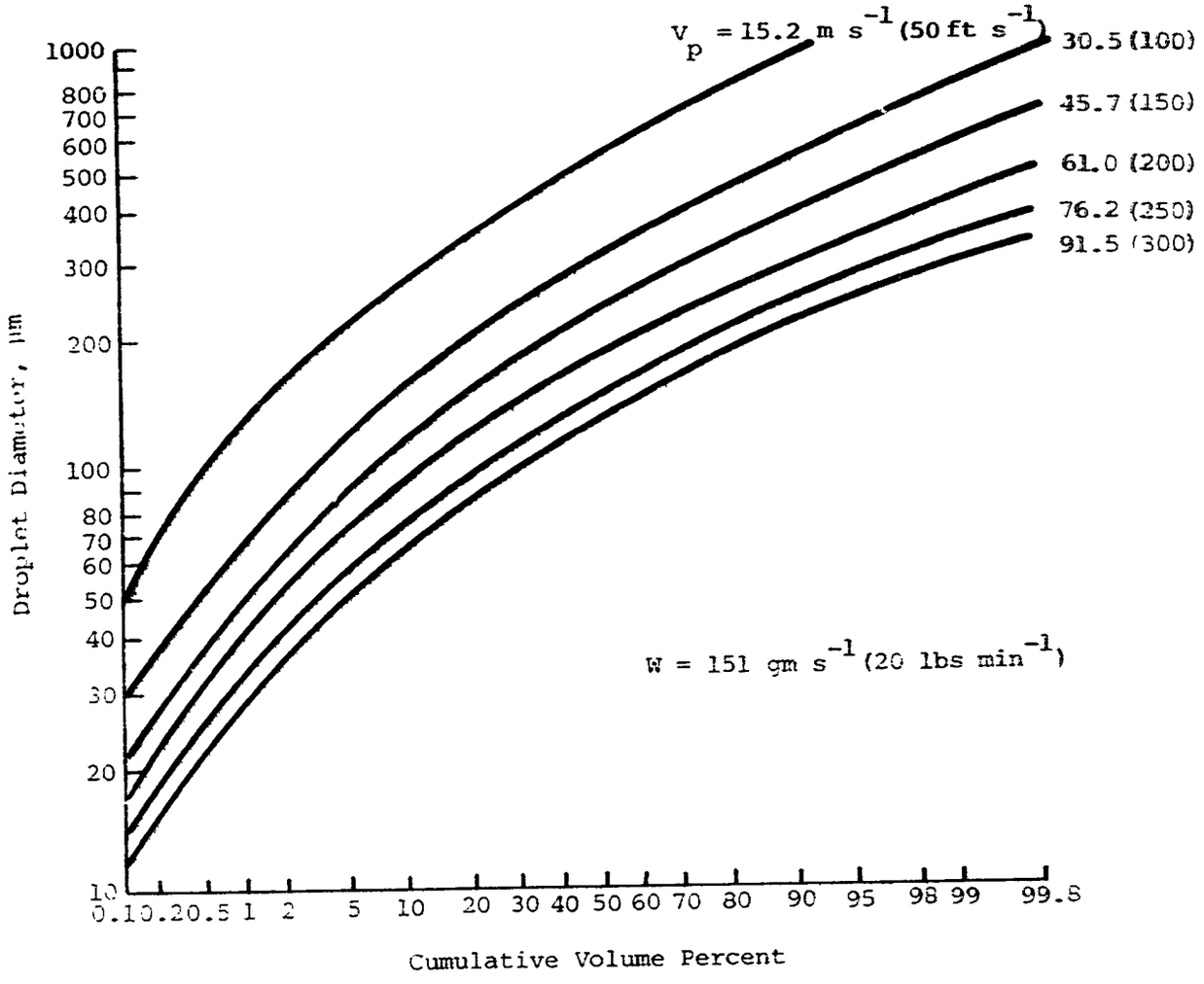

Figure 2.11 Drop size distributions from vaned disks for various peripheral speeds.

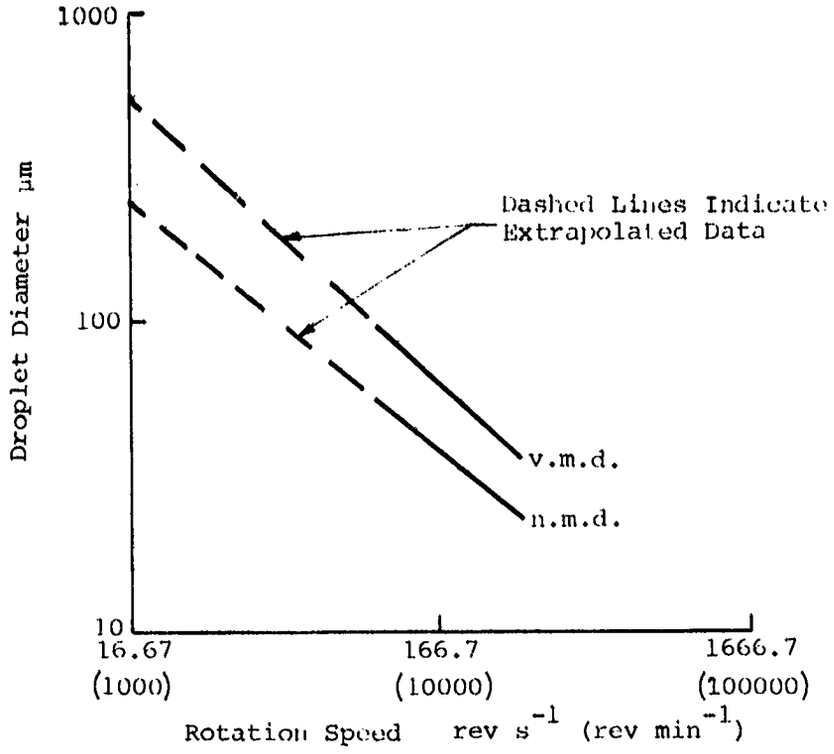

Figure 2.12 Number and volume median droplet diameters versus rotation speed at 0.2 ml s^{-1} (12 ml min^{-1}).

TABLE 2.1. SYNOPSIS OF DROPLET SIZE INFORMATION FROM SEVERAL ROTARY ATOMIZERS.

Rotation Speed		Restriction Washer Number	Flow Rate		v.m.d. (μm)	n.m.d. (μm)	Ratio v.m.d. n.m.d.
rev s^{-1}	rev min^{-1}		ml s^{-1}	ml min^{-1}			
250	15,000	1	0.0066	0.4	48	26	1.9
250	15,000	2	0.0250	1.5	40	23	1.7
250	15,000	3	0.0667	4.0	40	29	1.4
250	15,000	4	0.1417	8.5	41	32	1.3
250	15,000	5	0.2167	13.0	44	32	1.4
250	15,000	6	0.4333	26.0	45	33	1.4
250	15,000	7	0.7000	42.0	48	33	1.5
250	15,000	8	1.0000	60.0	64	37	1.7
200	12,000	1	0.0066	0.4	69	30	2.3
200	12,000	2	0.0250	1.5	62	31	2.0
200	12,000	3	0.0667	4.0	56	27	2.1
200	12,000	4	0.1417	8.5	54	33	1.6
200	12,000	5	0.2167	13.0	54	33	1.6
200	12,000	6	0.4333	26.0	52	39	1.3
200	12,000	7	0.7000	42.0	57	41	1.4
200	12,000	8	1.0000	60.0	60	38	1.6
150	9,000	1	0.0066	0.4	82	75	1.1
150	9,000	2	0.0250	1.5	80	32	2.5
150	9,000	3	0.0667	4.0	71	36	2.0
150	9,000	4	0.1417	8.5	64	40	1.6
150	9,000	5	0.2167	13.0	65	37	1.8
150	9,000	6	0.4333	26.0	71	50	1.4
150	9,000	7	0.7000	42.0	79	48	1.6*
150	9,000	8	1.0000	61.0	81	55	1.5†

*Mean of five measurements.

†Mean of four measurements.

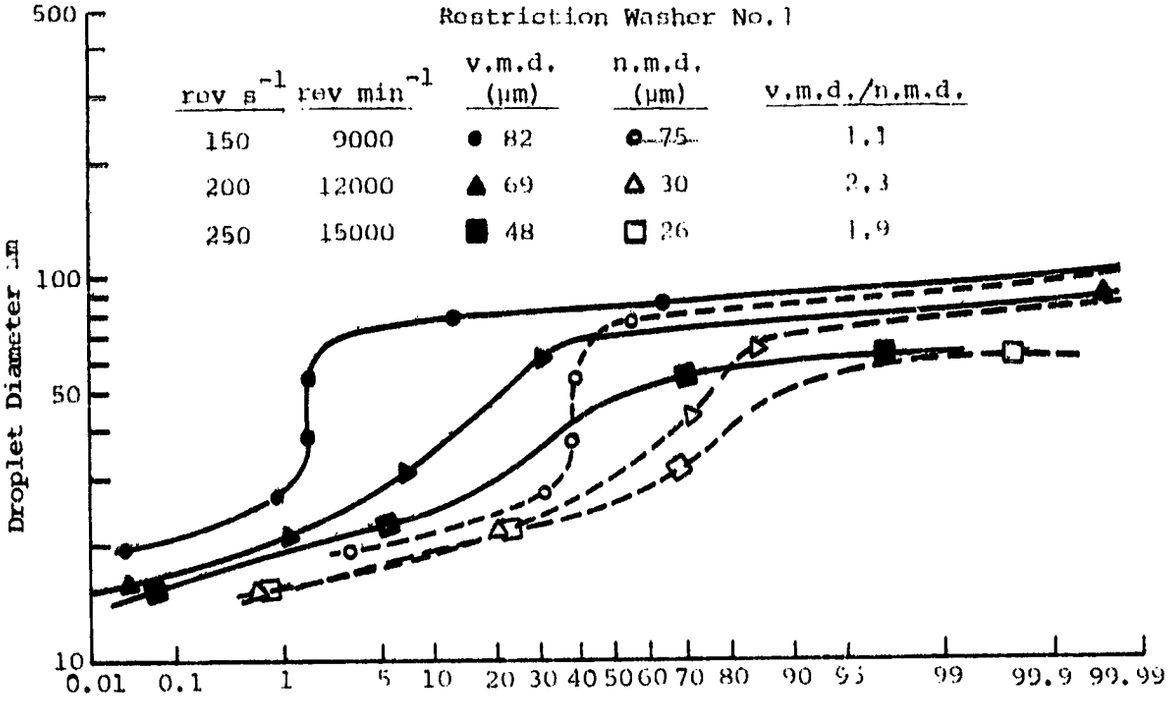

Figure 2.13 Droplet distribution using a rotary atomizer and restriction washer #1.

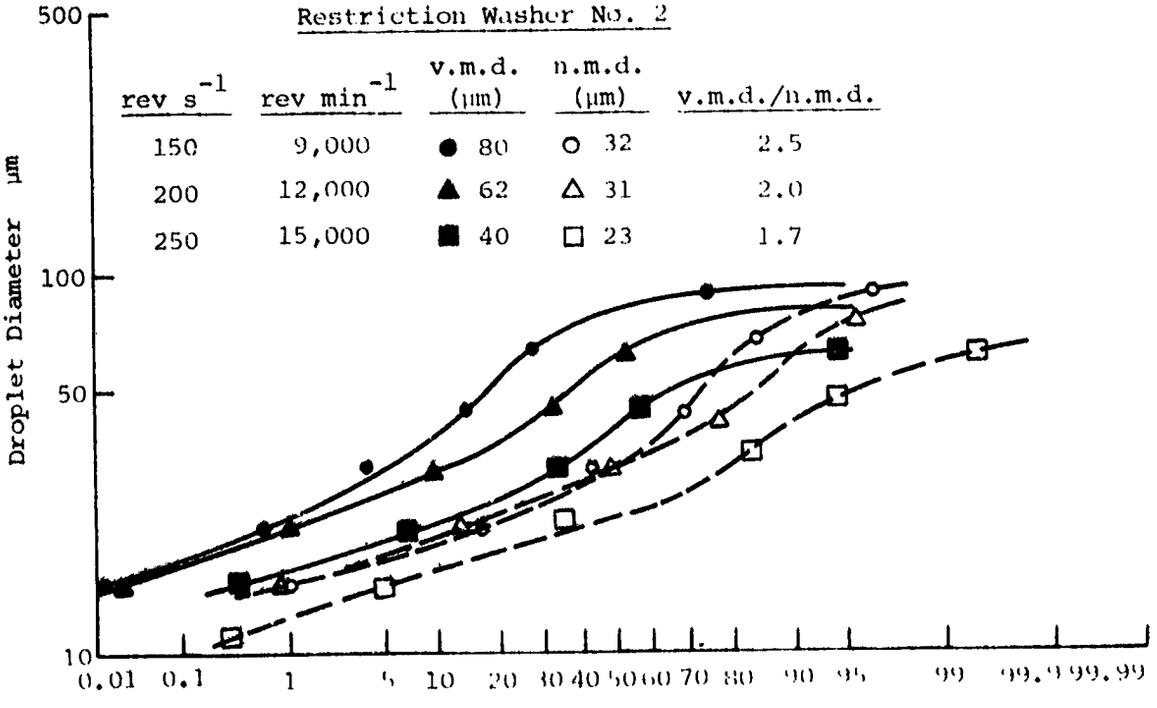

Figure 2.14 Droplet distribution using a rotary atomizer and restriction washer #2.

speed, the droplet size tends to fall and then rise again as the flow rate is increased. There exists a particular flow rate at which minimum size droplets are produced. This flow rate also tends to give the most uniform droplet size distribution. It appears that the variation of droplet size with flow rate is due to changes in the type of atomization. At low flow rates, particularly at 9,000 revolutions per minute, the distribution is typical of direct droplet formation (classical rotary atomization) with a main peak of droplets and a subsidiary peak of much smaller satellite droplets. As rotation speeds and flow rates increase, direct droplet formation gradually changes to ligament formation indicated by the log normal form of the distribution obtained. When flow rates are increased further, the droplet size range becomes wider as the ligaments thicken and start to break up into a combination of ligament and film (sheet) atomization due to excessive feeding of the rotor. Figures 2.15 and 2.16 illustrate the drop distribution uniformity of some typical rotary devices. Drop size distributions produced by rotary devices are, in general, more uniform than those produced by hydraulic or air atomizing nozzles.

Rotary atomization techniques show good potential for production of "monodisperse" droplets over a wide range of droplet sizes. This technique is assigned a rating of 4.15. Rotary atomization has been chosen as one of the two conceptual ideas for further development. Design details are presented in Section 4.0 of this report.

2.6 Monodisperse Droplets by Means of a Disintegrating Liquid Jet

Although jet stability (Newtonian) has been the object of numerous experimental and theoretical studies, the total problem of jet disintegration is by no means solved. It is true, however, that various details of the overall stability process have been worked out to a reasonable degree of completion. However, there are many missing parts in the description of the series of events commencing in a liquid reservoir and terminating with a breakup of a free jet. For example, the influence of ambient pressure, turbulence in the nozzle, fluid characteristics, and the degree of velocity profile development have not been adequately investigated. A brief literature survey of jet disintegration techniques will now be presented.

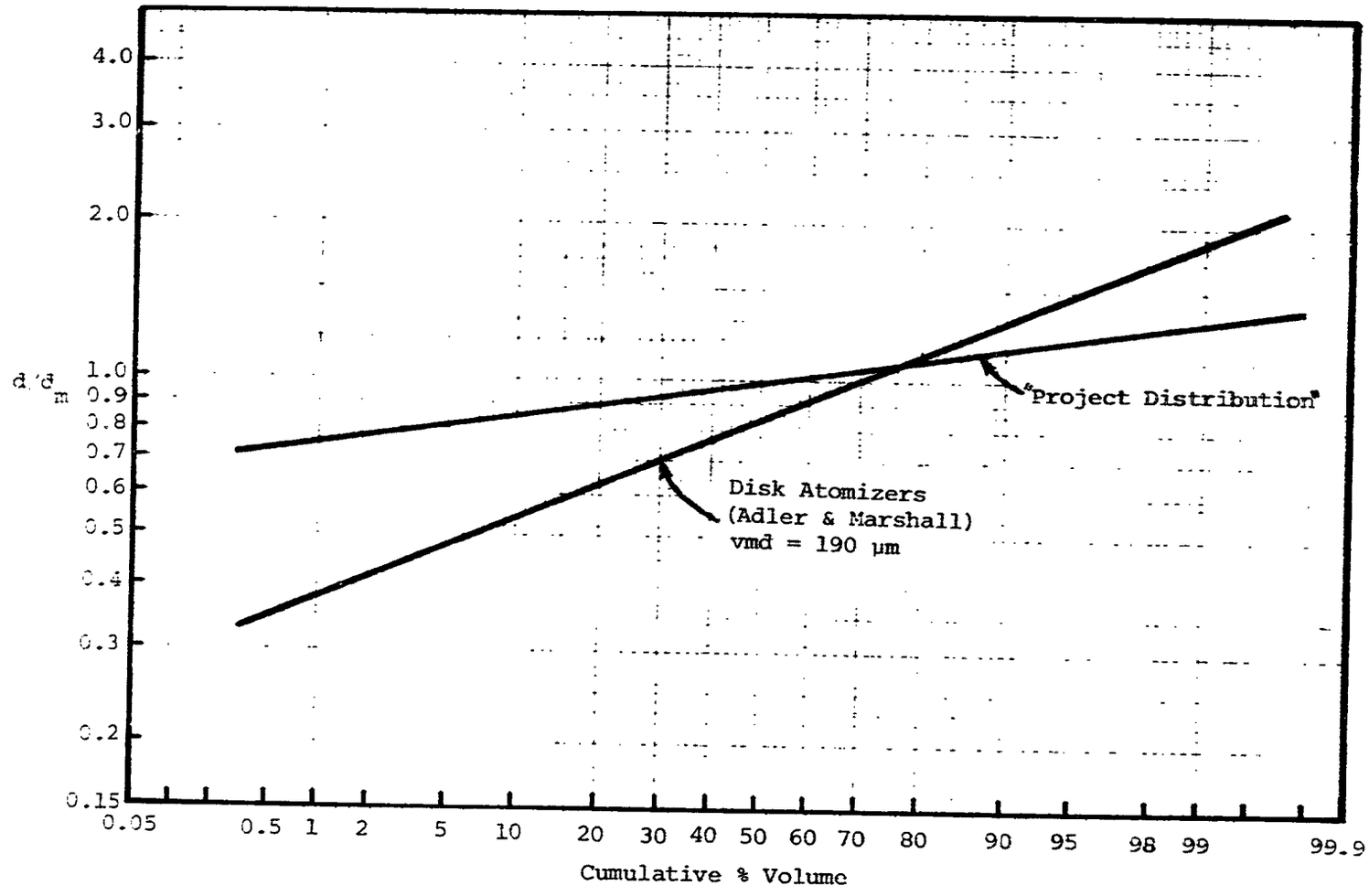

Figure 2.15 Drop size distribution--rotary atomizers.

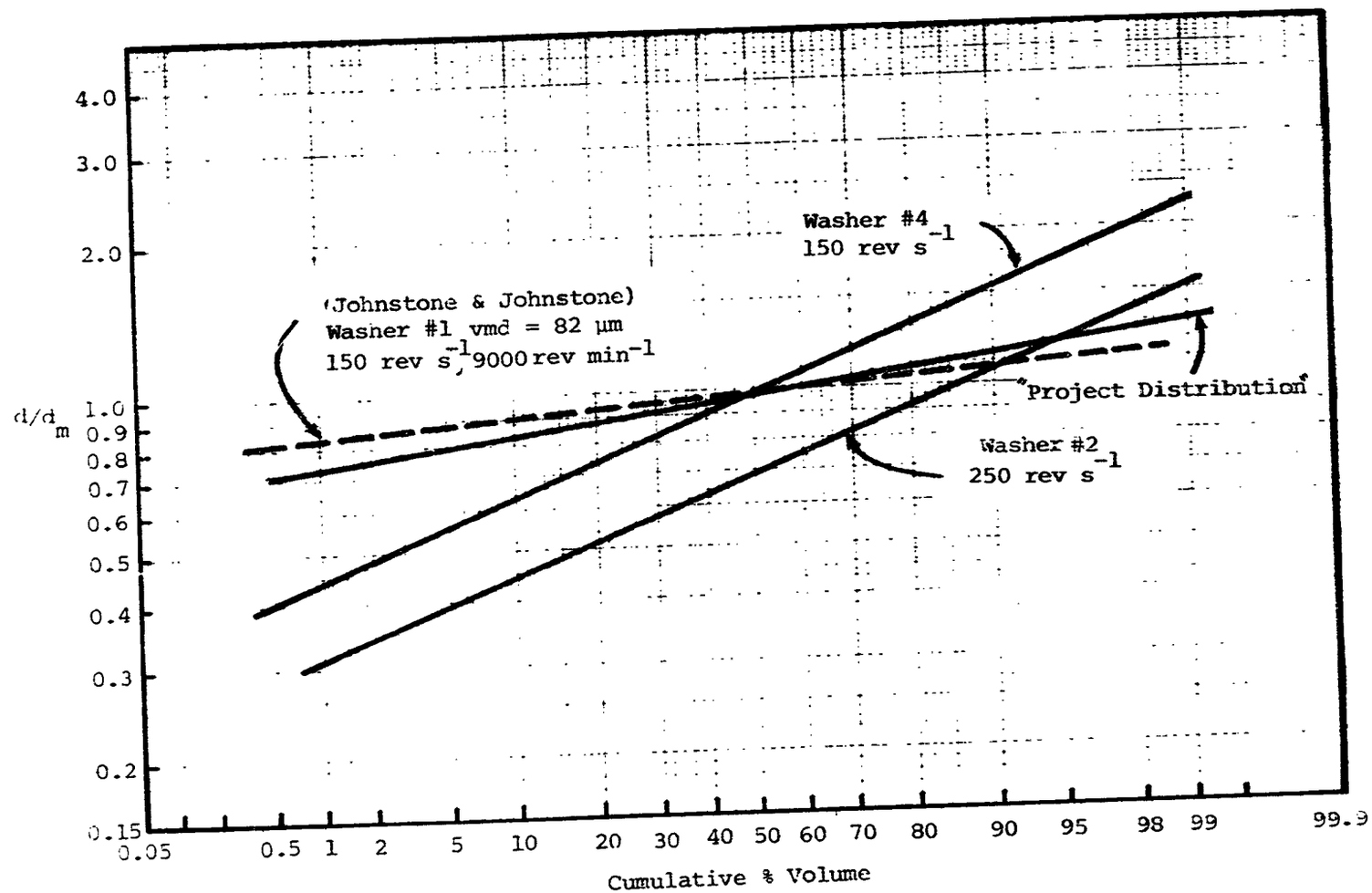

Figure 2.15 Drop size distributions--disk atomizers.

2.6.1 Survey of Jet Disintegration

The problem of describing jet disintegration has been the object of theoretical and experimental investigations beginning with the work reported by Savart [13]. Subsequent to Savart's experimental work, Plateau [14] and Rayleigh [15] contributed substantial quantitative descriptions of the stability mechanism. From potential energy considerations, Rayleigh was able to show that a cylindrical jet in a vacuum is stable with respect to all classes of infinitesimal disturbances except one. Specifically, the equilibrium configuration will always be unstable to a symmetrical disturbance whose wavelength exceeds the circumference of the cylinder.

Assuming an inviscid liquid, Rayleigh obtained an equation for the growth rate of a given symmetrical disturbance. By assuming the maximum growth rate, Rayleigh obtained an expression for the wavelength and growth rate of the destructive disturbance. His theory was in agreement with Savart's experimental observations. The scope of this description was quite narrow, however, for it did not take into account either the viscosity of the liquid or the possible influence of the ambient medium on the stability process.

Weber [16] guided by the experimental work of Haenlien, obtained a quantitative description of viscous jet stability. By a tedious but straightforward process, Weber showed that the break up length was a linear function of velocity for any given liquid and nozzle. For a viscous liquid, all other factors being equal, the predicted disintegration time exceeded that obtained by inviscid theory.

Although surface tension propagates only symmetrical disturbances, Weber succeeded in showing that aerodynamic forces tend to propagate both symmetrical and transverse disturbances. Weber then re-examined the symmetrical breakup of a viscous jet. More recent experimental studies of Dombrowski and Hasson [17] and of Miesse [18] delineate the influence of various features such as ambient pressure on stability.

2.6.2 Analysis and Drop Size Distributions

As a starting point for this review of jet stability, a theoretical analysis [16] of the stability of a Newtonian jet is presented. Further details are presented in Section 4.0 of this report.

First, it is assumed that a surface disturbance, $\eta(z,t)$, may be written as a Fourier series involving terms of the form

$$\bar{\eta}(z,t) = \bar{\eta}_o e^{\alpha t + ikz} \tag{2-1}$$

in a coordinate system fixed to the jet, where α is the growth rate, k is the wave number, z is the axial distance, t is the time, and $\eta(z,t)$ is the amplitude of the surface disturbance whose origin, z = 0, is at the tube exit at t = 0. Weber [16] assumes that the disturbances are symmetric about the jet axis and sufficiently small so that inertial forces could be neglected. After considerable manipulation, a characteristic equation for the growth rate α was found.

If the ambient fluid is assumed to exert neither radial nor shear stresses (jet in a vacuum or low speed jet in gas), the equation obtained is

$$\alpha^2 F_1 + \alpha F_2 \frac{3\mu\zeta^2}{\rho a^2} = \frac{\sigma}{2\rho a^3}(1 - \zeta^2)\zeta^2 \tag{2-2}$$

where F_1 and F_2 are ratios of Bessel functions whose arguments include α and k. It can be shown that the curve of α versus ζ ($\zeta = 2\pi a/\lambda = ka$) goes through a maximum, and hence there is a disturbance at some wave number which grows most rapidly.

The jet is assumed to be subject to a spectrum of disturbances of the form of Equation 2-1, but to suffer disruption under action of the disturbance with the largest growth rate α^*. It is also assumed that break up occurs when the disturbance is comparable to the jet radius and the break up time is given by

$$\bar{\eta}(0,t) = a = \bar{\eta}_o e^{\alpha^* T} \tag{2-3}$$

where T is the breakup time, or

$$T = \left(\frac{1}{\alpha^*}\right) \ln\left(\frac{a}{\bar{\eta}_o}\right) \tag{2-4}$$

The breakup length is $L = vT$ or

$$L = \left(\frac{v}{\alpha^*}\right) \ln\left(\frac{a}{\bar{\eta}_o}\right) \tag{2-5}$$

where v is the jet velocity.

For low speed jets it is observed that $\zeta \ll 1$. It can be shown that the solution of Equation 2-2 can then be obtained with good approximation by setting $F_1 = F_2 = 1$. One can obtain α^* from the quadratic equation that results from Equation 2-2. Equation 2-5, in terms of dimensionless variables, becomes therefore

$$\frac{L}{D} = [\ln(a/\bar{\eta}_o)]\ (We^{1/2} + 3We/Re) \tag{2-6}$$

where We is the Weber number and Re is the Reynolds number. The parameter $\ln(a/\bar{\eta}_o)$ must be determined experimentally.

In a further analysis, Weber included the pressure effects of an inviscid atmosphere. The characteristic equation for α then becomes

$$\alpha^2 F_1 + \alpha F_2 \frac{3\mu\zeta^2}{\rho a^2} = \frac{\sigma}{2\rho a^3}(1 - \zeta^2)\zeta^2 + \frac{\rho_A v^2}{2\rho a^2}\zeta^3 F_3 \tag{2-7}$$

where F_3 is another ratio of Bessel functions with α and ζ in their arguments. When air effects are important, no approximations for F_1, F_2, or F_3 are permissible and Equation 2-7 must be solved numerically for α versus ζ. Figure 2.17 shows the breakup curve for ethlene-glycol. The experimental work was accomplished by [19] and is illustrated by solid triangles. The most interesting feature of Weber's analysis of symmetrical breakup is that it predicts a maximum in the length-velocity curve. This suggests that, at least, the form of the equation is essentially correct.

A typical drop size distribution which can be produced by a vibrating orifice device is shown in Figure 2.18. This technique is assigned an overall rating of 3.90. The vibrating orifice device has been chosen as one of the two conceptual ideas for further development. Design details are presented in Section 4.0.

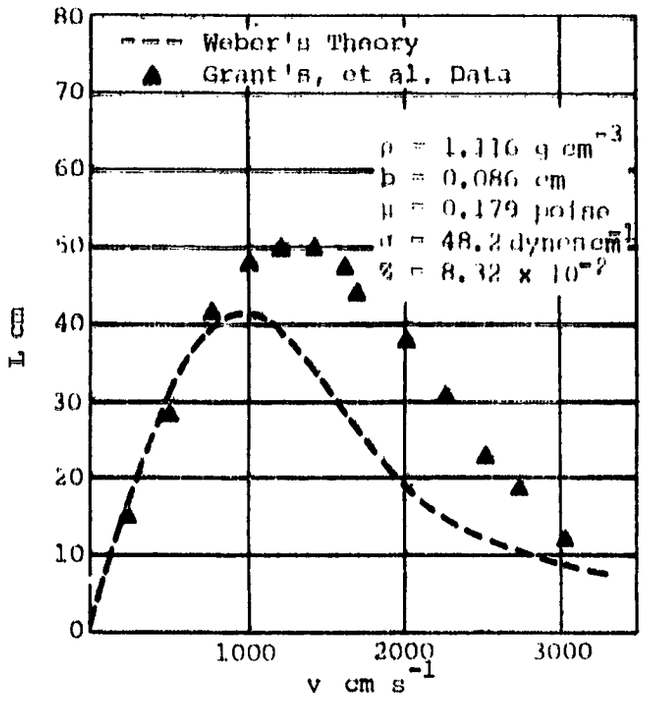

Figure 2.17 Breakup curve for ethylene-glycol.

2.7 Rating Summary of the Different "Monodisperse" Atomization Techniques

A number of different atomization techniques have been investigated. Each technique has been rated to indicate its overall potential for possible agricultural aerial applications. The rating was carried out using the following weighting factors: monodispersity, range of droplet sizes, application rates, practicality, simplicity, and economic viability. A compilation of the ratings for each technique is presented in Table 2.2.

Rotating and vibrating orifice devices have shown the greatest potential, over the range of fluid characteristics of agricultural chemicals, to produce a monodisperse droplet spray for agricultural applications. A more thorough analysis and assessment of these two techniques is presented in Section 4.0.

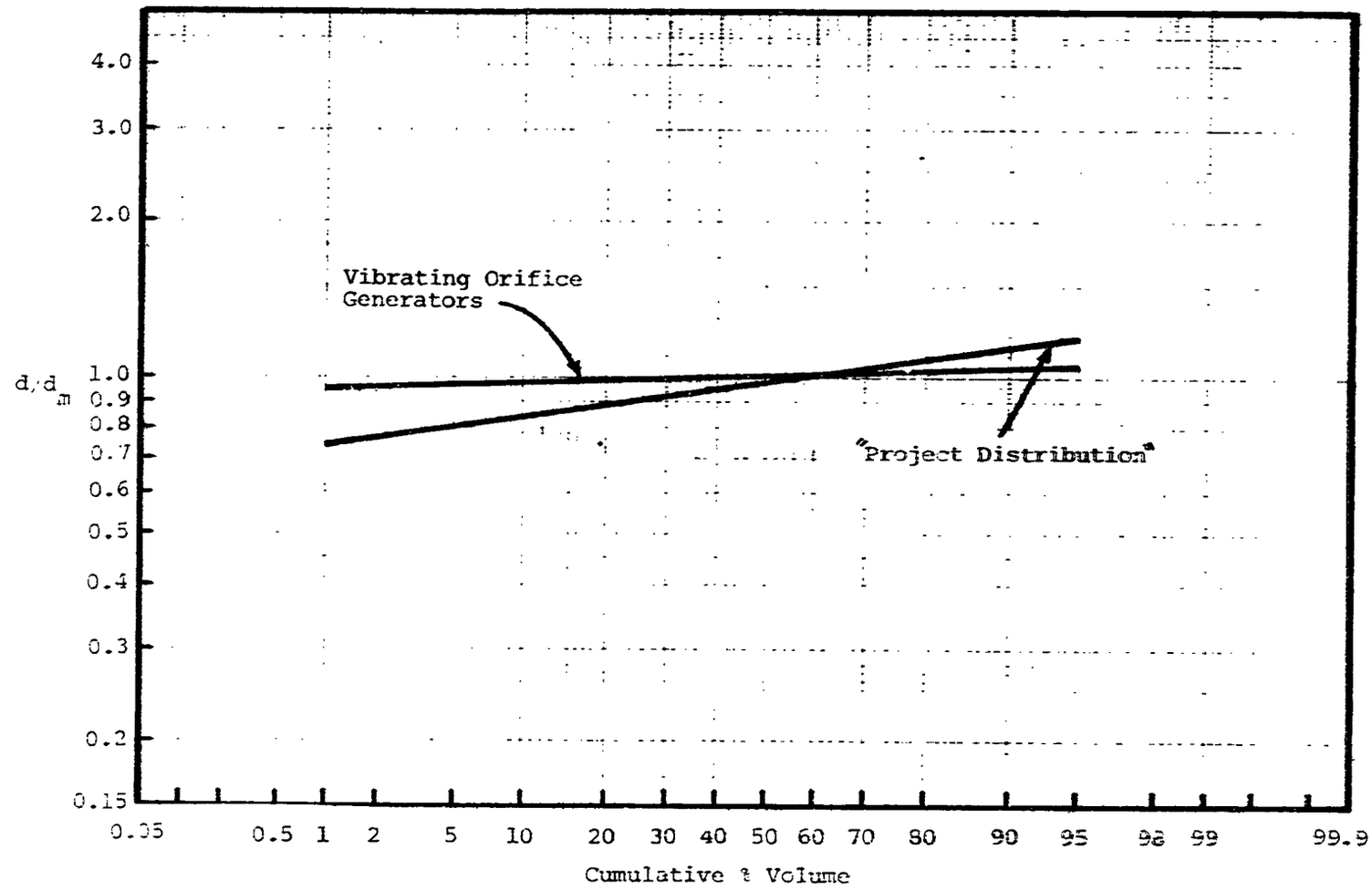

Figure 2.18 Typical droplet distributions--vibrating orifice generators.

TABLE 2.2. RATING COMPILATIONS.

Technique	Discussed in Report Section	Weighting Factors (Rating)						Overall Rating
		Monodispersity (30%)	Producible Droplet Sizes (25%)	Application Rate (15%)	Practicality (15%)	Simplicity (10%)	Economic Viability (5%)	
1	2.1	4	0	0	0	0	2	1.30
2	2.2	2	2	0	0	0	1	1.15
3	2.3	4	4	0	1	0	1	2.40
4	2.4	2	0	3	3	2	2	1.80
5	2.5	3	5	4	5	4	5	4.15
6	2.6	5	5	3	2	2	4	3.90

3.0 PHYSICAL CHARACTERISTICS OF AGRICULTURAL SPRAY APPLICATIONS

Today the predominate pesticide formulation used for pest control and applied by aircraft is sprays. The basic physical properties of these liquid formulations which affect the atomization process are the viscosity, surface tension, density, and vapor pressure. An agricultural operator can control, to some extent, the mean droplet diameter and, to a lesser extent, the uniformity by varying the above mentioned parameters. The typical range of chemical characteristics has been delineated and the new conceptual nozzle designs will be based on these ranges of physical properties. The ranges of physical properties which cover the majority of chemicals presently used are: viscosity, 1 to 10 centipoise; density, 0.8 to 1.2 g cm^{-3}; and surface tension, 20 to 73 dynes cm^{-1}. Each parameter will be briefly discussed in this section.

3.1 Viscosity

One of the most important liquid properties which effects droplet size and distribution uniformity is the viscosity. An increase in viscosity dampens any natural instabilities in liquids which then delays disintegration and increases the droplet diameter. Figure 3.1 illustrates the effect that viscosity (rotary-type atomizer) can have on droplet size. The two liquid viscosities used were 10 and 45 centipoise (cp).

Table 3.1 shows the variation in physical properties of some liquids and chemicals used for spray applications. The viscosity of the majority of agricultural spray solutions ranges from approximately 1.0 cp for water to 10 cp for some oils used for weed control. The viscosity of liquids generally decreases with an increase in temperature. In general, the chemical manufacturers do not determine all of the physical properties of the chemicals they produce. Literature searches have indicated that the density is the most widely measured property. There is a

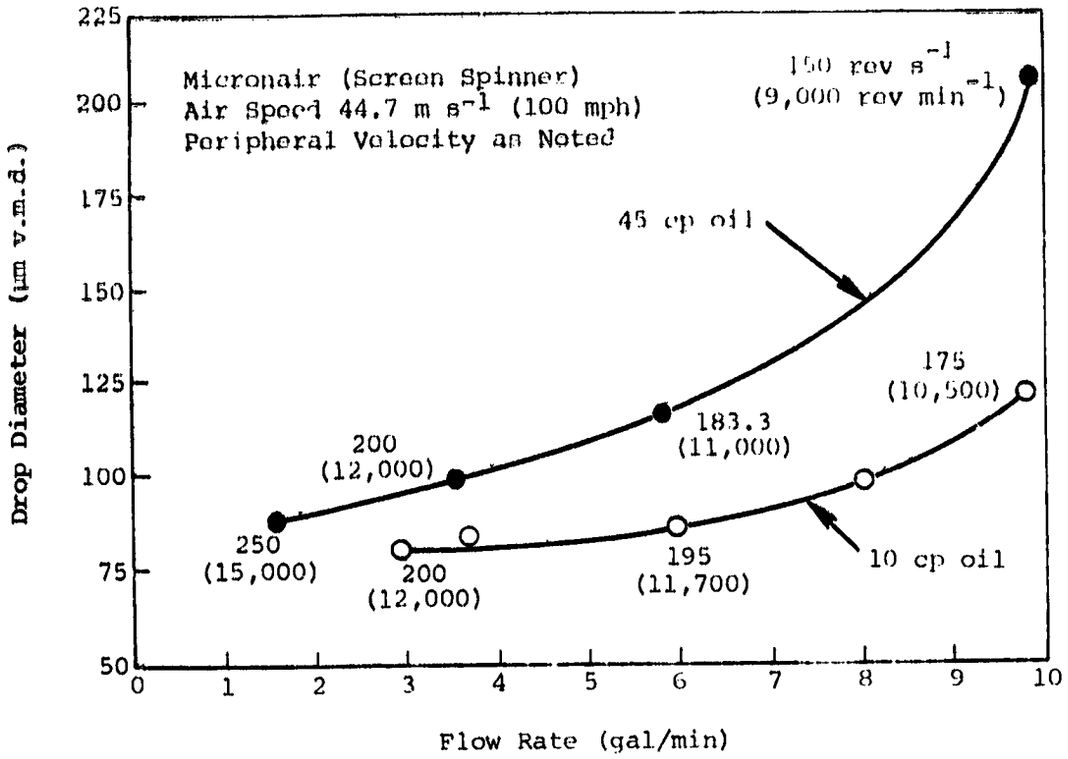

Figure 3.1 Droplet diameter versus liquid flow rate. Data for two liquid viscosities are illustrated.

complication introduced into the atomization problem due to the fact that a good number of agricultural chemicals and solutions (principally adjuvants) are non-Newtonian.

The viscosity of complex or non-Newtonian (nonlinear relationship between shear stress and shear strain rate) fluids is a function of the shear rate. In recent years, several new adjuvants (non-Newtonian) used to modify the viscosity of agricultural sprays have been introduced.

Preliminary investigations [20] indicate that an increase in droplet size and to some extent uniformity can be obtained with the appropriate use of adjuvants. Most of the formulations produce non-Newtonian solutions, and consequently it is necessary to specify the shear rate with the viscosity. Some of the non-Newtonian chemicals or adjuvants which are presently being used in agricultural applications are listed in Table 3.2 [21]. The apparent viscosity reduction with shear rate points

TABLE 3.1. VARIATION IN PHYSICAL PROPERTIES--SELECTED LIQUIDS AND CHEMICALS.

LIQUID	VISCOSITY	SURFACE TENSION	DENSITY
Castor oil	1000	39	0.970
Glycerol	800	63	1.260
SAE 30 (lube oil)	300	36	0.900
"Flozine"	30 - 320	--	---
SAE 10	100	36	0.900
Cottonseed oil	70	35	0.920
Malathion (95%)	45	32	1.230
Ethylene glycol	20	47	---
"Target"	5 - 15	--	---
Diesel fuel	10	30	0.890
Kerosene	2.50	25	0.820
Turpentine	1.49	--	0.870
Ethanol	1.20	22	0.790
Water	1.00	73	1.000
Methanol	0.60	22	0.800
Gasoline	0.35	--	0.680
Acetone	0.32	24	0.790
Parathion (ethyl)	--	--	1.350
DDT	--	--	1.40 (solid)
Dursban (75%)	--	--	0.970
Naled (85%)	--	--	1.965
Fenthion (93%)	--	--	1.25
Captan	--	--	1.73

TABLE 3.2. NON-NEWTONIAN THICKENING AGENTS.

Non-Newtonian Thickening Agents	Viscosity cp at 20° C, Showing Two Rates of Shear	
	1/50 sec	1/4,000 sec
Invert emulsion: 5% emulsifier, 10% diesel fuel, 85% water	700	16
Remaining mixtures each contain 2.5% Tordon (herbicide) in total of 100 gallons water and mix		
Norbak 6.2 lbs.	680	45
Vistik 6.5 lbs.	450	16
Keltex 8.5 lbs.	260	39
Dacagin 6.0 lbs.	140	13

out the desirable effect of lower pressure losses through the lines and nozzles. This reduction is also desirable because non-Newtonian fluids have less effect on droplet formation if a high shear rate is produced in the liquid film formed by the nozzle. Very little secondary breakup will occur once the drops are formed due to the increase in apparent viscosity at the lower shear rate. The type of generator used will critically effect the drop size distribution produced. The viscosity must, therefore, be measured under different operating conditions, such as nozzle pressure and flow rate. Information, however, of this kind is practically nonexistent. There are fragments of this type of information available at agricultural research facilities and some manufacturers' research laboratories. Figure 3.2 gives the viscosity of "Flozine" in terms of spindle rate of a centrifugal device. The chemical Flozine is a suspending agent for herbicide, insecticide, and fungicide wettable powders. Figure 3.3 gives the viscosity of "Target" as a function of spindle rate. "Target" is a drift reduction agent which is reported to increase the droplet size and uniformity of the spray.

Dimensionless products of the governing variables, such as the Weber number (ratio of the inertial force to the surface tension force) and the Reynolds number (ratio of the inertial force to the viscous

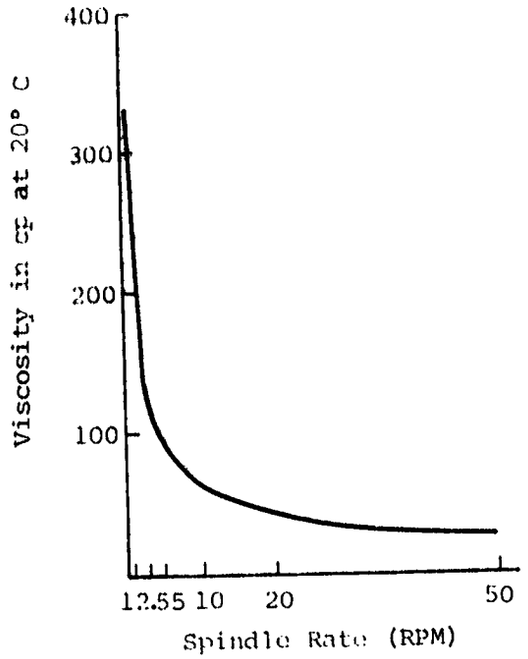

Figure 3.2 Viscosity as a function of spindle RPM - "Flozine."

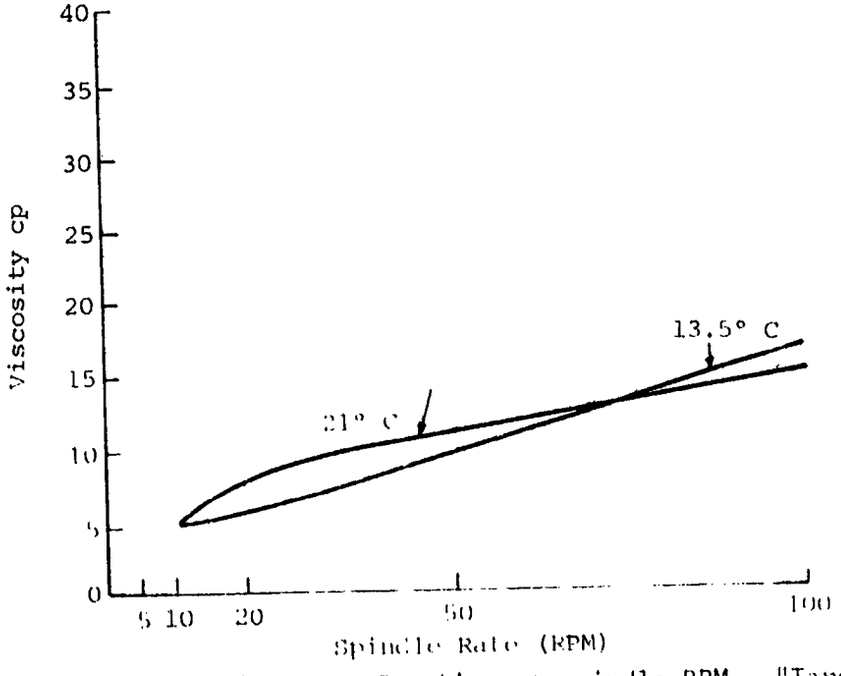

Figure 3.3 Viscosity as a function of spindle RPM - "Target."

force) have been used to relate the atomization for different fluids and operating conditions. More details concerning these dimensionless products are given in Section 4.0.

3.2 Surface Tension

Surface tension represents a direct force that resists the formation of a new surface area. The minimum energy required for atomization is equal to the surface tension multiplied by the increased liquid surface area. The Weber number, $We = \rho v^2 a/\sigma$ (where σ is the surface tension) has been shown to be one of the useful dimensionless products that may be related to the drop size whenever surface tension forces are important. Commonly encountered surface tensions range from 73 dynes per centimeter for water to as low as 20 dynes per centimeter for petroleum products. For most pure liquids, the surface tension in contact with air decreases with an increase in temperature and is independent of the age of the surface. Droplet production and drop size distributions are sensitive to variations in surface tension.

3.3 Density

Density usually has very little effect on atomization due to the small range of densities that are normally encountered in spray formulations. The density generally ranges from a low of approximately 0.8 g cm^{-3} to a high of 1.2 g cm^{-3}. The density may be indirectly affected by the spray pressure. However, this effect is small since the bulk modules of most liquids is high.

3.4 Vapor Pressure

The vapor pressure has little effect on the initial droplet size spectrum for most agricultural spray formulations. Table 3.3 illustrates some of the vapor pressure constants for some pesticides and carriers. Although the vapor pressure is unimportant in determining the initial drop size spectrum, it can have a significant influence on the evaporation of droplets and, therefore, a significant influence on the final droplet distribution impacting on the plant foliage.

TABLE 3.3. VAPOR PRESSURE OF SOME PESTICIDES AND CARRIERS.

MATERIAL	VAPOR PRESSURE (mm Hg)	Temperature (°C)
Water	4.58	0
Water	9.21	10
Water	12.79	15
Water	17.53	20
Water	23.76	25
Water	31.82	30
Water	55.32	40
Malathion	4.00×10^{-5}	30
Parathion	3.78×10^{-5}	20
2,4-D (acid)	10.50×10^{-3}	25
DDT	1.90×10^{-7}	20

The drop size distributions produced by most droplet generators used for agricultural applications are skewed normal (Gaussian). Typically, the percent (by volume) of small droplets decreases as the overall median diameter increases. An increase of viscosity or decrease in surface tension usually increases the droplet size and thus decreases the percent by volume of small droplets. Increased density usually produces small drops and increased vapor pressure or evaporation rate will reduce droplet size after production.

4.0 CONCEPTUAL IDEAS

After careful consideration of the range of fluid physical characteristics presented in Section 3.0, two conceptual ideas were selected as having the greatest potential for production of "monodisperse" sprays and for development into practical agricultural spray nozzles. The two conceptual ideas selected utilize the principles of vibration of a liquid jet with subsequent breakup and droplet formation by rotary atomization. Each of these two techniques will be analyzed in more detail in this section.

4.1 Vibrating Orifice Concept

Without any external disturbance, jets issuing from an orifice are naturally unstable and will breakup into droplets of nonuniform diameter. However, if a mechanical disturbance, at an appropriate frequency, is applied the breakup can be controlled and monodisperse droplets can be produced. The breakup process is controlled due to the fact that the growth of instabilities on the liquid jet are frequency dependent. By superimposing the appropriate frequency, which corresponds to the greatest growth rate, the droplet formation process can be controlled. Once the droplets are produced, however, the droplets must be adequately dispersed or random coalescence and shearing effects will act to establish a polydisperse distribution.

The basic theoretical analysis of jet instability has received considerable attention from the time of Rayleigh [22]. The particular analysis presented here [23, 24] closely models the realistic physical configuration envisioned for a spray nozzle design for agriculture applications. The jet is considered to be semi-infinite and the disturbances periodic. Also, the undisturbed jet is considered to have some finite constant speed. It is assumed in developing the model that a liquid column issues from an orifice at a given speed and the orifice is vibrated longitudinally at a known frequency. In order to obtain

monodisperse droplet distributions, the maximum growth must be utilized. This maximum growth rate is a function of jet speed, jet diameter, viscosity, density, and surface tension. The assumption is made that the surface tension is constant throughout the jet. The axial velocity of the jet is assumed to be constant throughout the jet. The axial velocity of the jet is also assumed to be constant over the cross section of the jet. The fact that the axial velocity of the jet is assumed to be constant over the cross section is probably a good approximation for the purpose of designing spray nozzles for agricultural applications. The breakup usually occurs close enough to the orifice so that the jet velocity is constant over a large portion of its cross section. An analysis of the stability of a viscous liquid jet with a variable axial velocity would require numerical integration making the analysis much more complicated, and significant improvement in the analysis would probably not be obtained.

4.1.1 Analysis

Consider a liquid jet of initial radius, a, issuing from an orifice into air with an initial axial velocity, v_0. Let the surface deflection of the jet from the mean radius be η, as shown in Figure 4.1. Let the instantaneous jet radius be $\phi(z,t)$ and its instantaneous velocity be $v(z,t)$. The complete set of one-dimensional Cosserat equations are [23]:

$$\frac{\partial \phi^2}{\partial t} + \frac{\partial}{\partial z}(v\phi^2) = 0 \tag{4-1}$$

$$\pi\rho\phi^2\left(\frac{\partial v}{\partial t} + v\frac{\partial v}{\partial z}\right) = -\frac{\partial q}{\partial z} + 2\pi\sigma\left(\frac{\phi}{\sqrt{1+\left(\frac{\partial \phi}{\partial z}\right)^2}}\right) + \pi\rho g\phi^2 + 2\mu\pi\frac{\partial}{\partial z}\left(\phi^2\frac{\partial v}{\partial z}\right) \tag{4-2}$$

$$\frac{1}{8}\pi\rho\phi^4\left(\frac{\partial^2 v}{\partial z\partial t} + v\frac{\partial^2 v}{\partial z^2} - \frac{1}{2}\left(\frac{\partial v}{\partial z}\right)^2\right) = -q + \pi\sigma\left(\frac{\phi}{\left(1+\left(\frac{\partial \phi}{\partial z}\right)^2\right)^{1/2}}\right.$$

$$\left. - \frac{\phi^2\left(\frac{\partial^2 \phi}{\partial z^2}\right)}{\left(1+\left(\frac{\partial \phi}{\partial z}\right)^2\right)^{3/2}}\right) + \frac{1}{8}\mu\pi\frac{\partial}{\partial z}\left(\phi^2\frac{\partial^2 v}{\partial z^2}\right) - \mu\pi\phi^2\frac{\partial v}{\partial z} \tag{4-3}$$

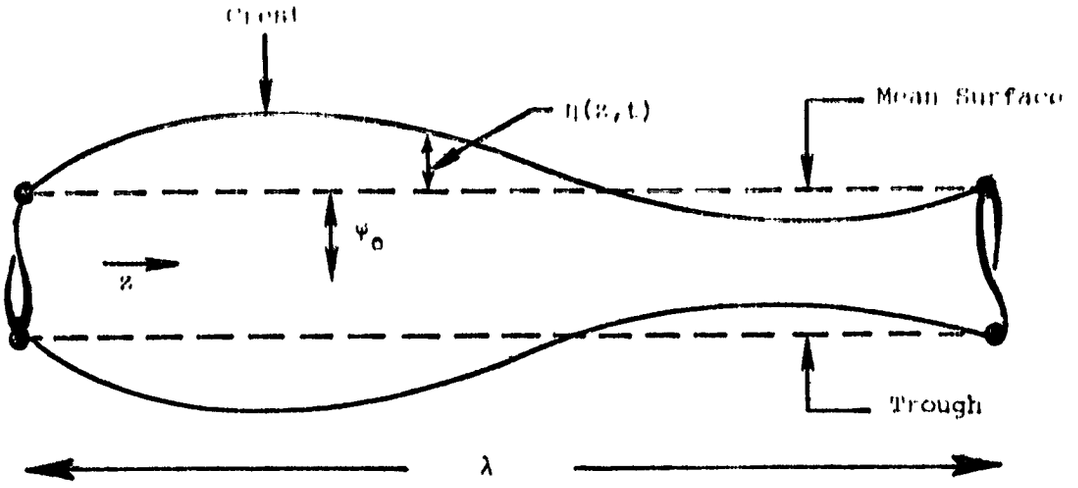

Figure 4.1 Surface deflection of a jet from the mean radius.

where

$$q = p - \pi p_0 \phi^2$$

In the above equations ρ, μ, σ, and g are the liquid density, viscosity, surface tension, and gravitational acceleration, respectively, and p_0 is the constant external surface pressure.

Nondimensionalizing lengths by a, time by a/v_0, velocity by v_0, and pressure by $\rho a^2 v_0^2$ and introducing the perturbation variables

$$\eta = \phi - 1$$

$$w = v - 1$$

into Equations 4-1 through 4-3 and eliminating the pressure between Equations 4-2 and 4-3 and linearizing, results in the following equations.

$$2\frac{\partial \eta}{\partial t} + 2\frac{\partial \eta}{\partial z} + \frac{\partial w}{\partial z} = 0 \qquad (4\text{-}4)$$

$$\frac{\partial w}{\partial t} + \frac{\partial w}{\partial z} - \frac{1}{8}\frac{\partial^2}{\partial z^2}\left(\frac{\partial w}{\partial t} + \frac{\partial w}{\partial z}\right) = \frac{1}{We}\frac{\partial}{\partial z}\left(\frac{\partial^2 \eta}{\partial z^2} + \eta\right) + \frac{1}{Re}\frac{\partial^2}{\partial z^2}\left(\rho w - \frac{1}{8}\frac{\partial^2 w}{\partial z^2}\right) \qquad (4\text{-}5)$$

In the above equations, Re is the Reynolds number defined as

$$Re = \frac{\rho a v_0}{\mu}$$

and We is the Weber number defined by

$$We = \frac{\rho a v_o^2}{\sigma}$$

For practical spray nozzle designs, it is desirable to relate the frequency of oscillation of the orifice, it being controllable, to the droplet size. The stability analysis will, therefore, be given in terms of time harmonic disturbance, rather than the conventional spatially harmonic functions. Thus, the analysis at this point will be a little different than the classical techniques and will be more applicable to the problem at hand.

Since Equations 4-4 and 4-5 are linear, partial differential equations with constant coefficients, a normal mode solution is applicable. The solution can be written in terms of temporally harmonic functions in the following way.

$$\begin{aligned} w &= w \exp[i(\omega t - kz)] \\ \eta &= \eta_o \exp[i(\omega t - kz)] \end{aligned} \qquad (4\text{-}6)$$

where ω is the frequency of oscillation which is a real number and k is complex. The real part of k is related to the wavelength and the imaginary part represents a spatial attenuation (or growth) in the axial direction. Upon substituting Equation 4-6 into Equations 4-4 and 4-5 one obtains the following algebraic equation

$$\frac{i}{8Re} k^5 - \left(\frac{1}{2We} - \frac{1}{8} + \frac{i\omega}{8Re}\right) k^4 - \left(\frac{\omega}{4} - \frac{3i}{Re}\right) k^3 + \left(\frac{1}{2We} + 1 + \frac{\omega^2}{8} - \frac{3i\omega}{Re}\right) k^2$$

$$- 2\omega k + \omega^2 = 0 \qquad (4\text{-}7)$$

for the growth rate in terms of the oscillation frequency.

In the inviscid limit, $Re \to \infty$, Equation 4-7 becomes

$$We(\omega - k)^2 = 4(k^2 - 1)k^2/(8 + k^2)$$

which compares to Pimbley's analysis [25] based on Lee's [26] one-dimensional analysis. The fifth order complex polynomial (Equation 4-7) can be evaluated numerically.

Empirical equations which relate the droplet size to the jet diameter, viscosity, density, and surface tension have also been developed. These empirical equations accurately estimate the size of droplets that will be produced. These equations are much simpler and easier to analyze than the theoretical equations considered above. The empirical equations have been used to evaluate the effects of fluid characteristics on the droplet size distributions. A more detailed analysis of theoretical jet breakup will be held in obeyance at this time and some of the more practical aspects of the conceptual design will be emphasized.

Rayleigh [22] was one of the first to do experimental research and develop empirical relationships. His analysis showed that the growth rate of a disturbance is maximized when the wavelength of the disturbance is 4.508 times the diameter of the jet. The effects of surface tension or density of the liquid were not considered. Weber [27] extended Rayleigh's analysis to include the effect of fluid characteristics and jet stream velocity. He found theoretically that the optimum wavelength for the growth of a disturbance on the surface of a jet stream could be expressed as

$$\lambda = \pi d_j \left(2 + \frac{6\mu}{(d_j \rho \sigma)^{1/2}}\right)^{1/2} \tag{4-8}$$

where d_j is the jet diameter; μ is the liquid viscosity; ρ is the liquid density; and σ is the surface tension. The diameter of the droplet can be assumed to be equal to 1.89 times the jet diameter [28]. Substitution into Equation 4-8 yields an equation relating the optimum wavelength for growth of an instability to the drop diameter (d), density, viscosity, and surface tension. The resulting relation is given by

$$\lambda = \pi \left(\frac{d}{1.89}\right) \left(2 + \frac{6\mu}{\left(\frac{d\sigma\rho}{1.89}\right)^{1/2}}\right)^{1/2} \tag{4-9}$$

The frequency of the cyclic instability can be determined using the relationship $f = v/\lambda$ where v is the jet velocity, hence

$$f = \frac{V}{\pi\left(\frac{d}{1.89}\right)\left(2 + \frac{6\mu}{\left(\frac{d\rho\sigma}{1.89}\right)^{1/2}}\right)^{1/2}} \qquad (4\text{-}10)$$

The steady state equilibrium equation for a vibrating, orifice-type generator can be expressed as [28]

$$d = \left(\frac{6Q}{\pi f}\right)^{1/3} \qquad (4\text{-}11)$$

where Q is the flow rate. Substitution of Equation 4-10 into Equation 4-11 yields, using cgs units;

$$d^{9/2} - \frac{17.92\, d^{1/2}}{V^2} - \frac{83.13Q^{1/2}\mu}{V^2(\rho\sigma)^{1/2}} = 0 \qquad (4\text{-}12)$$

which can be solved numerically. Figures 4.2 through 4.7 illustrate the effect of fluid characteristics on droplet size. The graphs indicate that over the range of fluid characteristics commonly encountered in agricultural chemicals that viscosity will have the greatest effect on droplet size. Surface tension and density have a less pronounced effect. The velocity of the jet and/or flow rate also effect the droplet size. As the velocity or flow rate increases, the variation in droplet size decreases. The variation in droplet size due to velocity or flow rate changes may be compensated for by varying the generator frequency to maintain the optimum breakup conditions.

Experimental measurements should verify that monodisperse droplets can be produced in sufficient quantities for agricultural applications using the vibrating orifice method. The question remains, however, as with any system, is the distribution which impinges on the foliage monodisperse or has such parameters as turbulence caused breakup or coalescence to occur creating a deposited distribution which is polydisperse? Such effects are probably present when dispersing chemicals from fixed- or rotary-wing aircraft. Measurements of the droplet distribution at the generator exit, using a nonevaporating fluid, and again just before impaction on the foliage would serve to illucidate this problem.

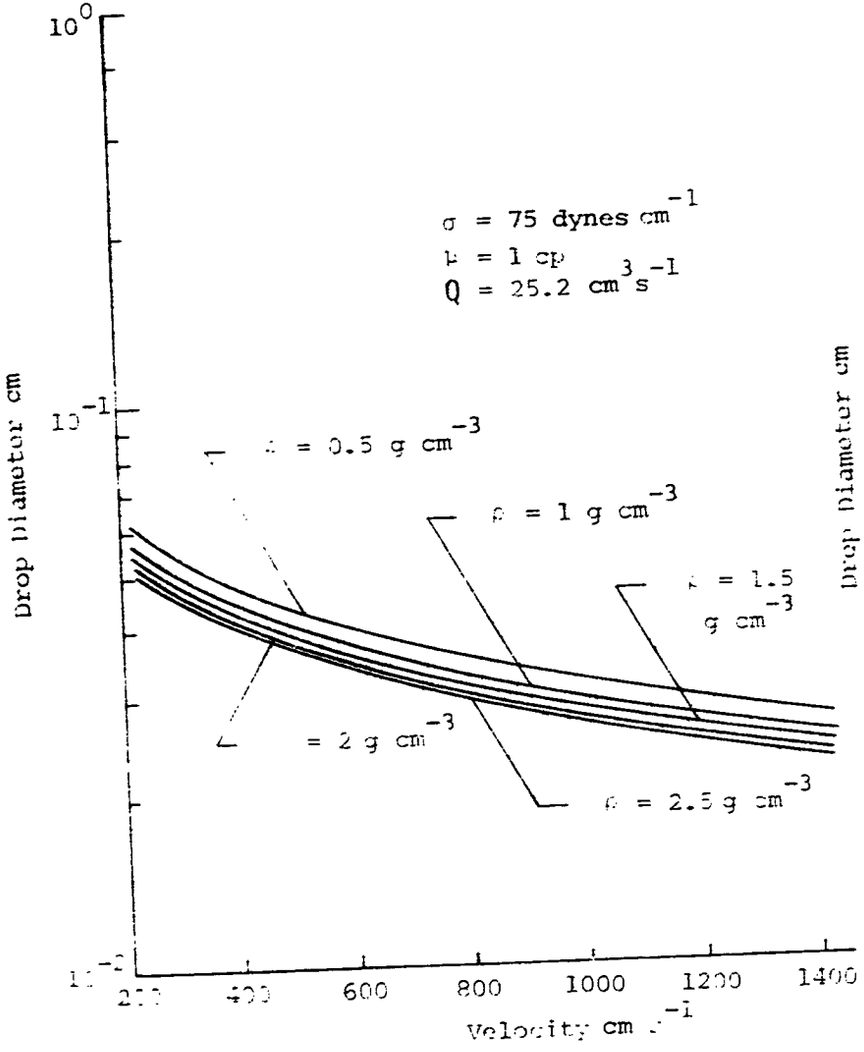

Figure 4.2 Drop diameter versus jet velocity. The effect of liquid density is presented.

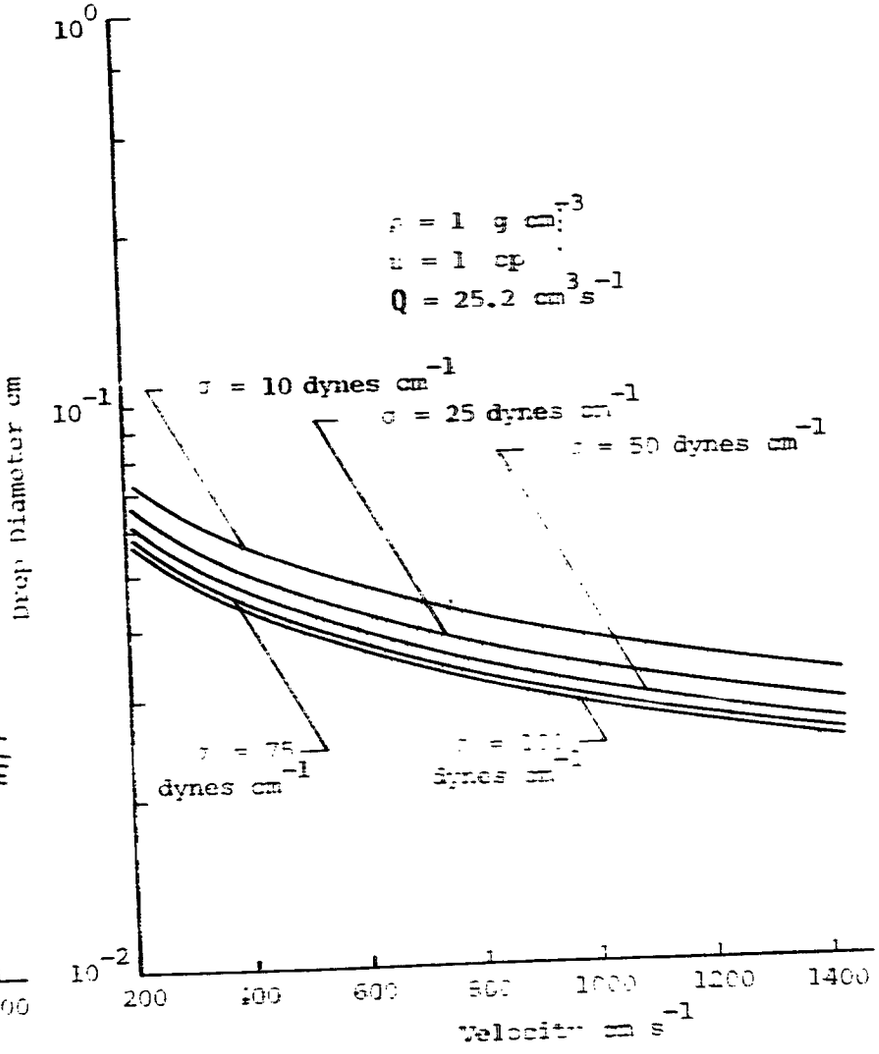

Figure 4.3 Drop diameter versus jet velocity. The effect of surface tension is presented.

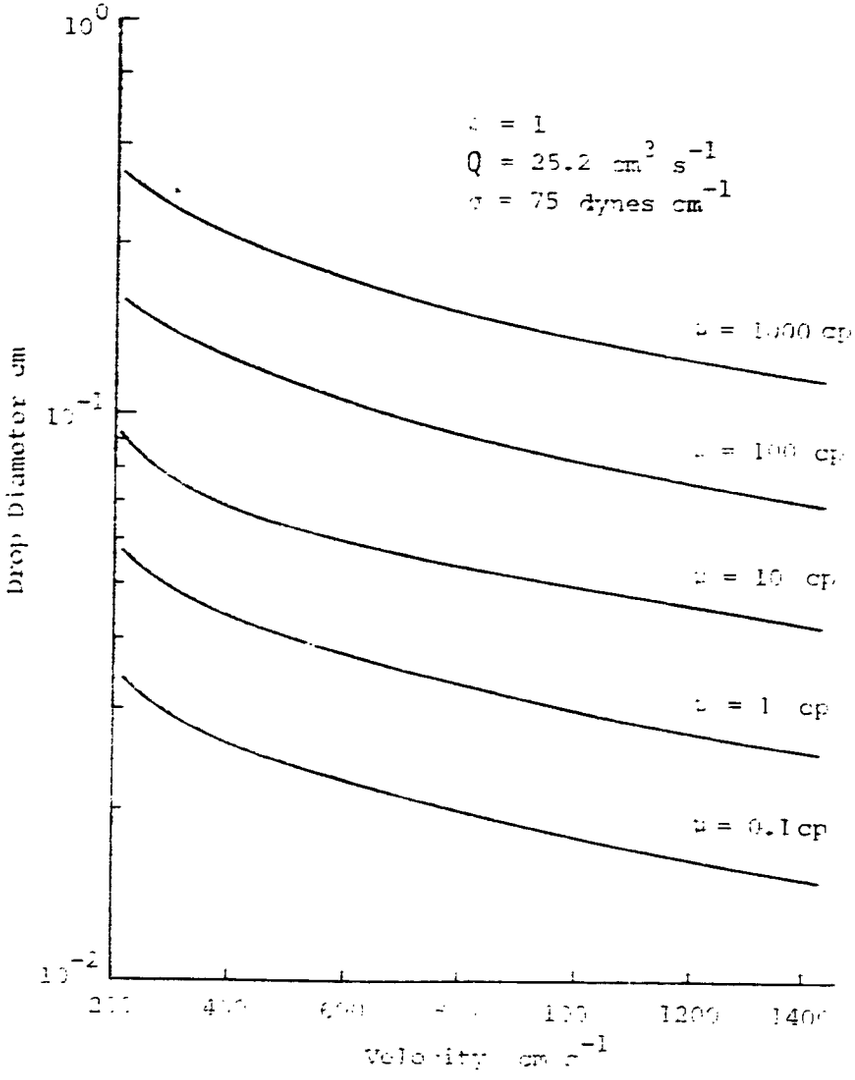

Figure 4.4 Drop diameter versus velocity. The effect of liquic viscosity is presented.

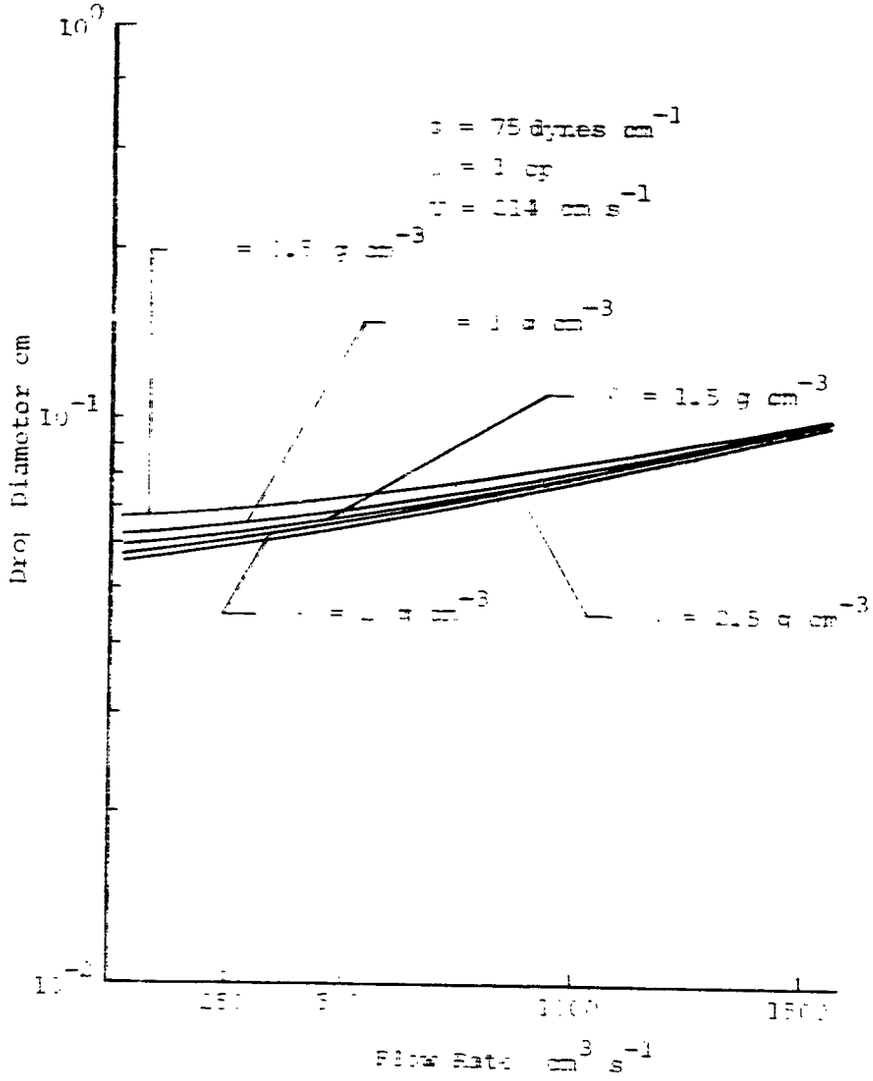

Figure 4.5 Drop diameter versus flow rate. The effect of liquid density is presented.

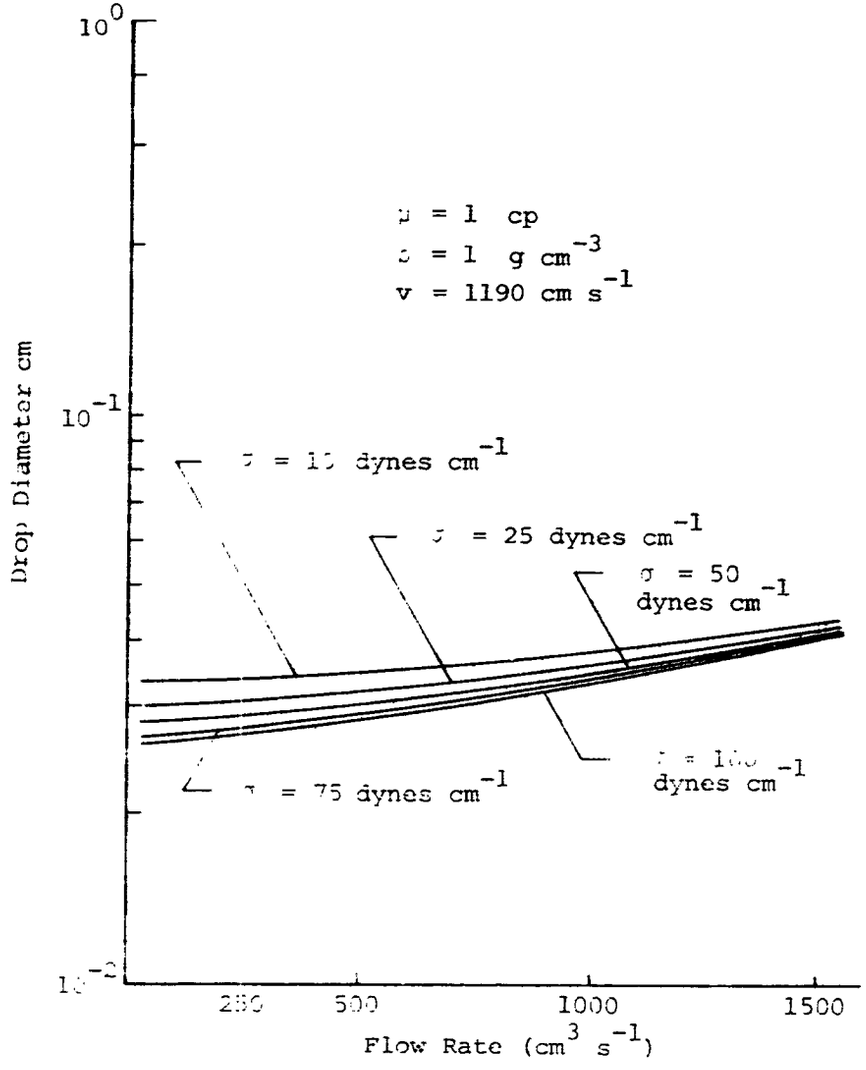

Figure 4.6 Drop diameter versus flow rate. The effect of surface tension is presented.

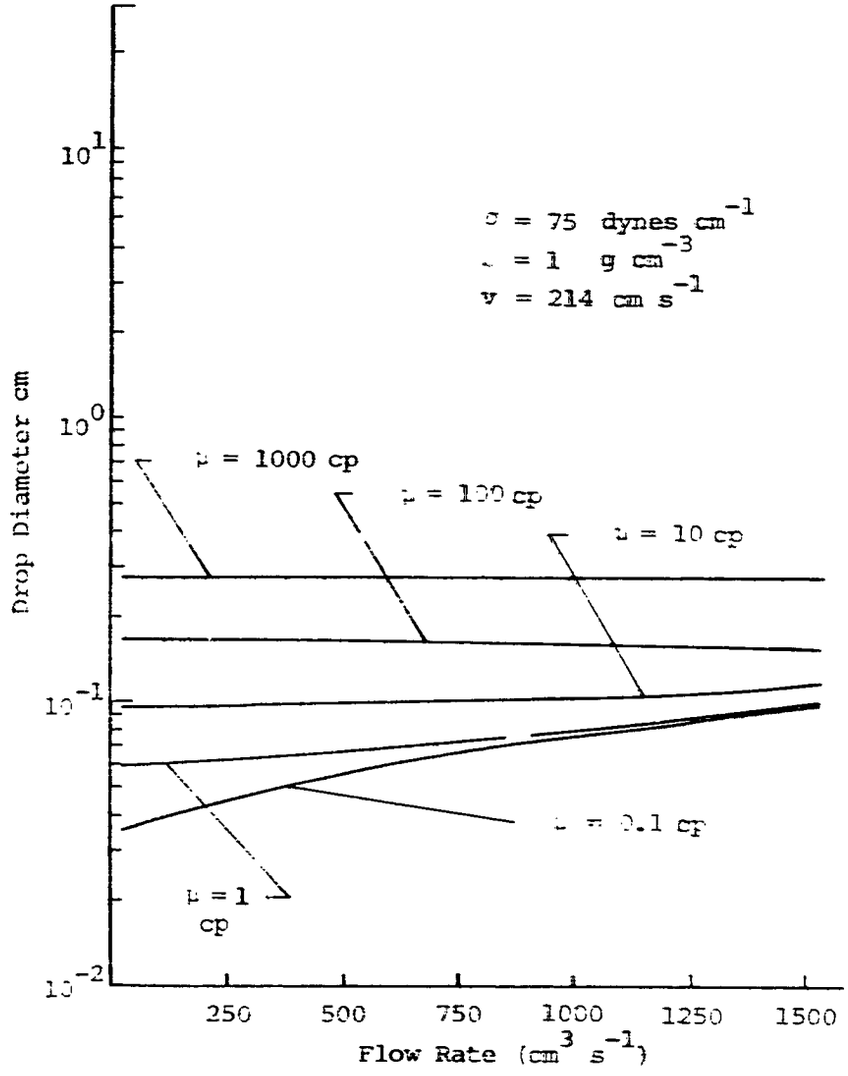

Figure 4.7 Drop diameter versus flow rate. The effect of liquid viscosity is presented.

4.1.2 Dispersal Method and Conceptual Design--Vibrating Device

In this section a description of the conceptual design and a method to disperse the particles will be very briefly summarized. With this type of device, a number of holes would be placed in a thin metal plate. Vibrations would be set up at the maximum instability growth rate frequency. Droplet concentrations will depend on such things as flow rate, fluid characteristics, and oscillation frequency. The drops would be dispersed using appropriately placed air jets. To further insure that no recombination effects were active, the drops could be unipolarly charged using a induction ring system. The ring could be placed immediately downstream of the droplet formation area and as near to the droplet formation area as possible. The dispersal system will, therefore, consist of monodisperse unipolarly charged droplets being produced and then dispersed using jets of air to clear the apparatus and settle to the vegetation unimpeded. A diagram illustrating one possible setup is presented in Figure 4.8. Detailed engineering drawings and hardware development should be the next phase of this endeavor.

4.2 Rotary Atomization Concept

4.2.1 General Description

One of the most promising methods of producing monodisperse droplets for agricultural applications is rotary atomization. Atomization using this method is achieved by supplying liquid to the center of a rotating disk, cup, or cage. In the conceptual design described in this section, the liquid is supplied through a stationary tube to the inner part of a rotating cup widening toward a rim. Friction between the liquid and the wall of the cup cause the liquid to attain the same rotational speed as that of the cup. Centrifugal forces set up in the liquid will cause a flow of liquid toward the rim of the cup and droplets to form at the periphery. At sufficiently high angular speeds of the cup, the layer of liquid formed at the inner wall of the cup is very thin. A schematic diagram illustrating the design is given in Figure 4.9.

Three essentially different droplet formation mechanisms may take place around and beyond the edge of the cup. Which one of these actually

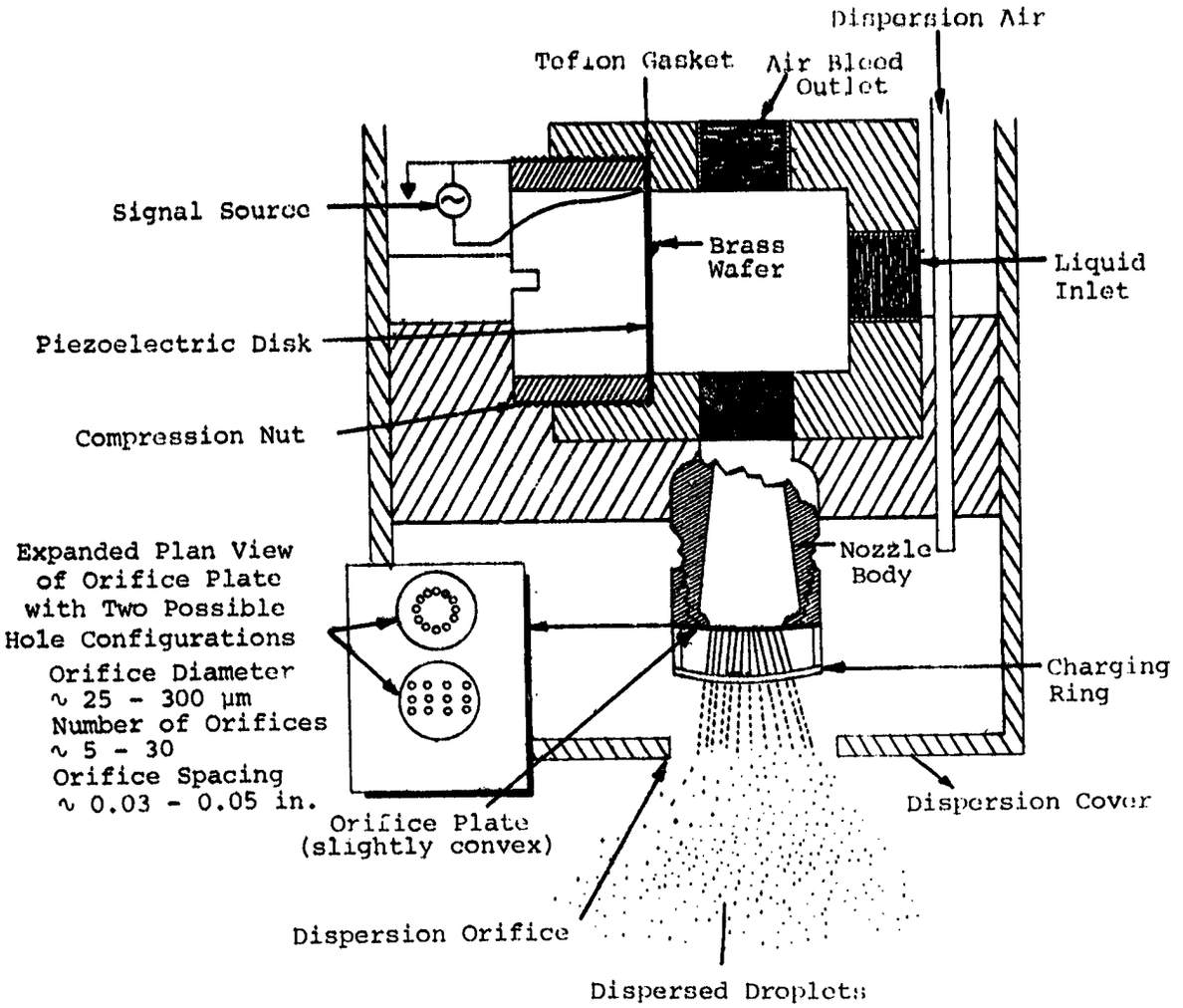

Figure 4.8 Diagram of vibrating-type device dispersal system showing location of orifice plate, air jets, piezoelectric vibrator, induction ring system, and two possible orifice configurations.

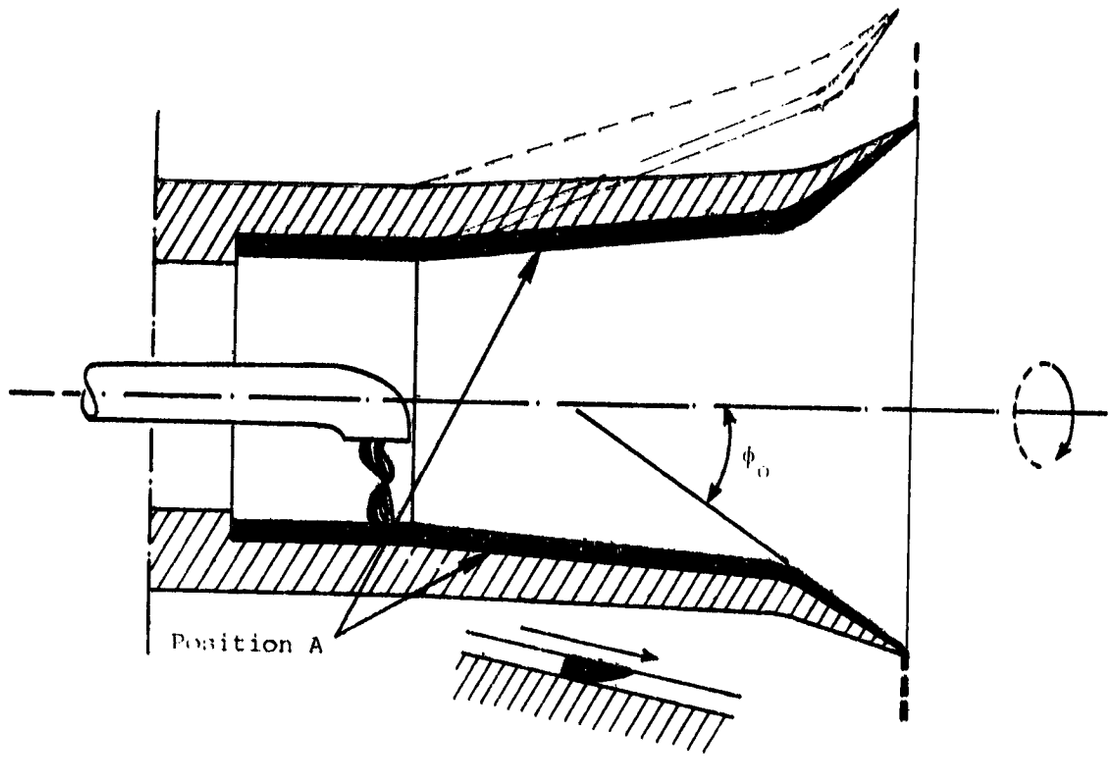

Figure 4.9 Schematic diagram illustrating the design of a rotary atomizer.

occurs depends on working conditions, i.e., liquid flow rate, angular speed, and dimensions of the cup; and on properties of the liquid, i.e., density, viscosity, and surface tension. For a brief description of these droplet formation mechanisms it is sufficient to cover the case of a cup rotating with a fixed angular speed while different quantities of liquid are supplied to the cup.

At very small liquid flow rates a torus is formed around the periphery of the cup. The diameter of this torus is determined principally by centrifugal and surface-tension forces. Single drops form at one or more bulges which form on the torus. These bulges or drops are then propelled from the periphery. Figure 4.10 illustrates this phenomenon which is commonly referred to as "disintegration by direct drop formation."

At increased flow rates, the formation of complete thin jets or ligaments occurs. The number of ligaments increases with increasing flow rate up to a maximum value, after which the number of ligaments

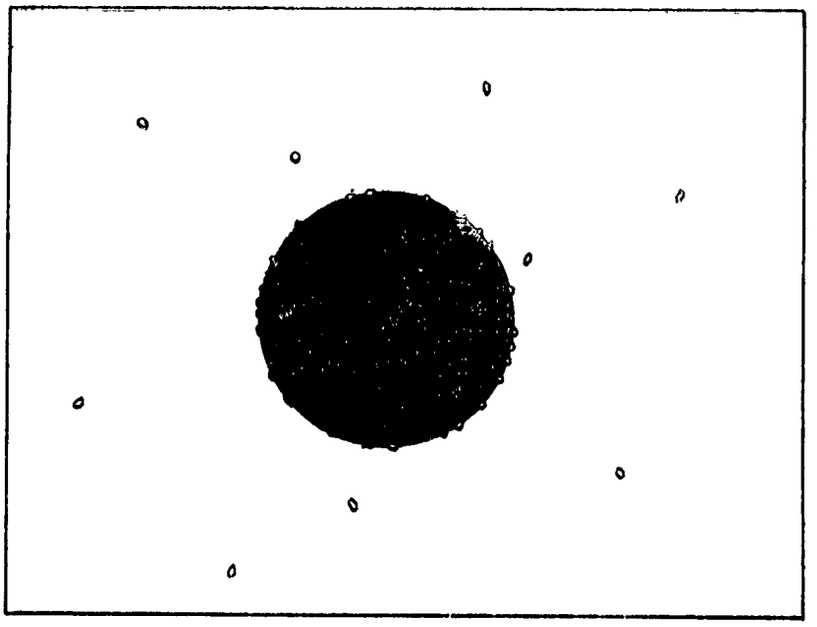

Figure 4.10 Disintegration by direct drop formation.

remains constant, irrespective of the flow rate. Apparently, in this flow rate region the ligaments grow in thickness with increasing flow rate. The ligaments themselves are unstable and break up into drops at some distance from the periphery of the cup. Figure 4.11 illustrates this phenomenon which is commonly referred to as "disintegration by ligament formation." A more detailed description of ligament formation is presented in Section 4.2.3.

By continuously increasing the flow rate, a condition is finally reached where neither the number nor thickness of the ligaments will increase. The ligaments are then unable to incorporate all the liquid supplied to the cup. The result is that the torus will be propelled from the periphery and a film will form extending to a distance from the periphery where it breaks up in an irregular manner. Figure 4.12 illustrates this phenomenon which is commonly referred to as "disintegration by film formation."

Droplet uniformity may be improved by producing a liquid layer of uniform thickness within the cup. This results in ligaments of equal

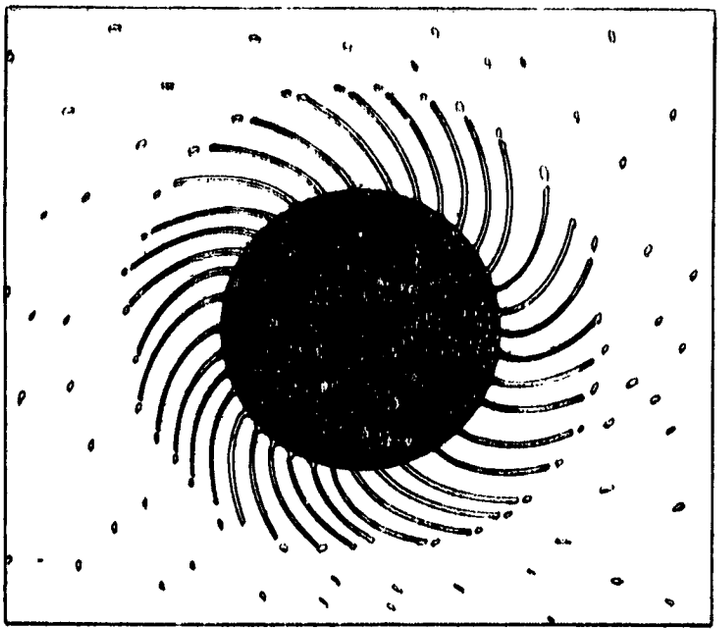

Figure 4.11 Disintegration by ligament formation.

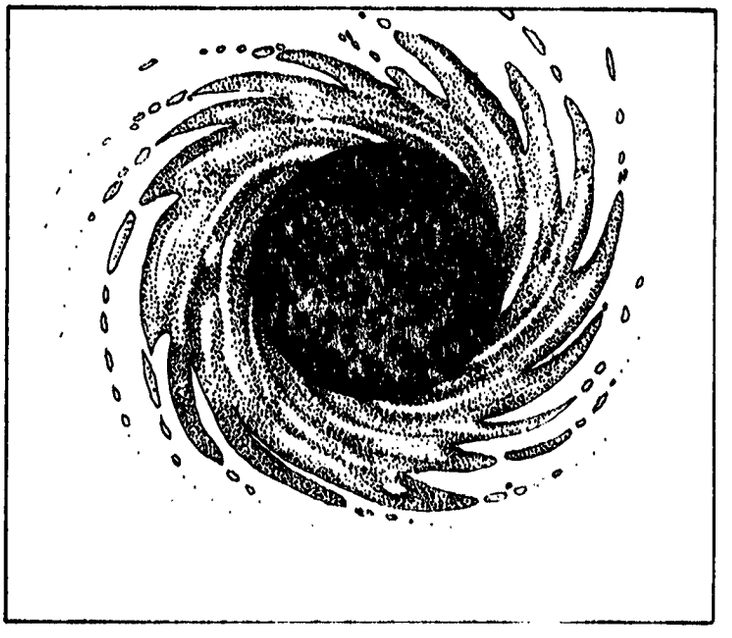

Figure 4.12 Disintegration by film formation.

thickness and spacing around the periphery. In order to insure a uniform liquid layer thickness, several requirements need to be satisfied.

a) Gravitational effects must be negligible; this means that centrifugal acceleration must be much greater than the gravitational acceleration ($\omega^2 r > 10\ g$)

b) Rotation must be completely free from vibrations

c) Liquid supply must be uniform.

Calculations of liquid flow in the cup will be presented in the following section.

4.2.2 Calculation of Liquid Flow in the Cup

This calculation of the liquid flow in the cup is based on the following assumptions:

a) The thickness of the layer is very small compared with the dimensions of the cup.

b) The flow within the layer is completely laminar.

c) The flow within the cup is rotationally symmetric.

By comparing the order of magnitude of the various terms occurring in the hydrodynamical equations for viscous flow, the following may be shown:

a) The static pressure, p, is practically constant across the layer.

b) The velocity component, v_ϕ, is very small with respect to the component v_ξ (see Figure 4.13).

c) The velocity component v_θ is very small with respect to the component v_ξ; this implies that the path described by any liquid particle with respect to the cup is practically straight and radial. The liquid has practically the same rotational speed as that of the cup.

Hence, with the assumption of a constant static pressure and neglecting the velocity components v_ϕ and v_θ, the equation of motion and the boundary conditions are (see Figure 4.13):

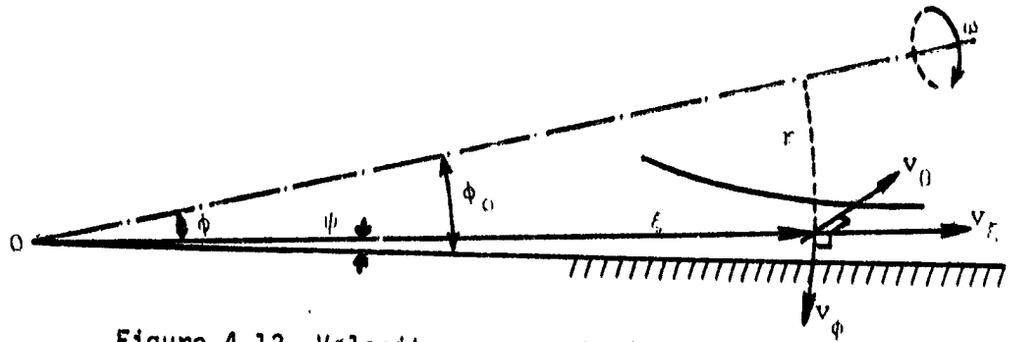

Figure 4.13 Velocity components in liquid layer in cup.

$$\frac{\partial^2 v_\xi}{\xi^2 \partial \psi^2} + \frac{\rho \omega^2 \xi}{\mu} \sin^2 \phi_o = 0 \tag{4-13}$$

$v_\xi = 0$ at the wall ($\psi = 0$)

$$\frac{\partial v_\xi}{\xi \partial \psi} = 0 \text{ at the free surface } (\psi = \psi_1) \tag{4-14}$$

The solution of the differential equation, which satisfies the boundary conditions, is

$$v_\xi = \frac{\rho \omega^2}{\mu} \sin^2 \phi_o \left(\xi_1^3 \psi_1 \psi - \xi^2 \frac{\psi^2}{2} \right) \tag{4-15}$$

where ξ_1 is the value of ξ at the free surface. The value ψ_1 is determined by the condition that the total quantity of liquid flowing through the layer toward the rim of the cup must be equal to the quantity Q supplied to the cup.

This condition gives

$$Q = \int_0^{\psi_1} 2\pi r \xi v_\xi d\psi = \frac{2\pi \rho \omega^2 \xi_1^5 \sin^3 \phi_o \cdot \psi_1^3}{3\mu} \tag{4-16}$$

$\xi_1 \psi_1 = \delta$

$\xi_1 \sin \phi_o = r$

$$Q = \frac{2\pi\rho\omega^2 r^2 \delta^3 \sin \phi_o}{3\mu} \tag{4-17}$$

$$\delta = \left(\frac{3\mu Q}{2\pi\rho\omega^2 r^2 \sin \phi_o}\right)^{1/3} \tag{4-18}$$

The values of the maximum radial velocity, $v_{\xi(1)}$, and of the mean radial velocity, $v_{\xi(m)}$, are, respectively

$$v_{\xi(1)} = \left(\frac{9\rho\omega^2 \sin \phi_o \, Q^2}{32\pi^2\mu r}\right)^{1/3} \tag{4-19}$$

and

$$v_{\xi(m)} = \left(\frac{\rho\omega^2 \sin \phi_o \, Q^2}{12\pi^2\mu r}\right)^{1/3} \tag{4-20}$$

The condition for the validity of the simplifications introduced is

$\psi_1 << 1$

or

$\frac{\delta}{\xi_1} << 1$

or

$$\left(\frac{\mu Q \sin^2 \phi_o}{\rho\omega^2 r^5}\right)^{1/3} << 1 \tag{4-21}$$

When the path described by a single liquid particle with respect to the cup is considered, it has been shown that this path is practically a straight line in the radial direction. For a stationary observer, however, the path is a spiral. An identical spiral will be described by liquid supplied at a stationary point to the cup. The shape of this spiral is determined by the ratio of the rotational speed ωr to the radial velocity v_ξ. Hence, the differential equation of the spiral, if described in terms of the coordinates ξ and θ, is

$$\frac{1}{r}\frac{d\xi}{d\theta} = \frac{v_\xi}{\omega r} \qquad (4\text{-}22)$$

Taking for v_ξ the value

$$v_\xi = k v_{\xi(1)}$$

where

$0 \leq k \leq 1$, the differential equation becomes

$$\frac{d\xi}{d\theta} = A\xi^{-1/3} \qquad (4\text{-}23)$$

where

$$A = k\left(\frac{9\rho Q^2}{32\pi^2\mu\omega}\right)^{1/3} \qquad (4\text{-}24)$$

The equation of the spiral is then

$$\xi = \left(\frac{4}{3}A\theta\right)^{3/4} \qquad (4\text{-}25)$$

where the constant of integration has been equated to zero.

4.2.3 Theoretical Analysis

The theoretical analysis is based on the processes occurring beyond the edges of the cup as described very roughly in the general description. The principal focus will be on the state of ligament formation.

It is assumed that a torus-like liquid ligament is formed around the edge of the cup, and from this torus the maximum number of ligaments originates. These ligaments grow in thickness with increasing quantity Q up to a maximum value, after which a transition into the state of film formation is likely to occur.

In order to estimate the thickness δ_t of the liquid torus, the simple reasoning presented below is followed. Figure 4.14 shows a plausible shape for the cross section of the torus.

In Figure 4.14, the liquid particles, after leaving the periphery of the cup, have: (a) a radial-velocity component v_D, which on the average

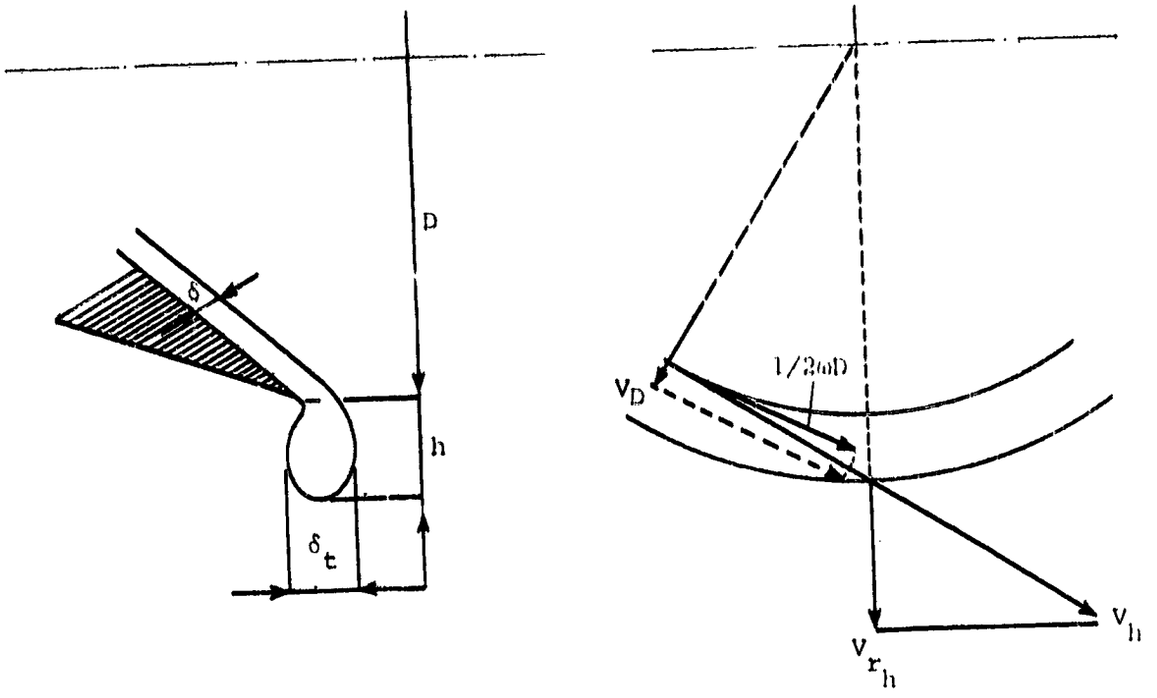

Figure 4.14 Flow conditions in the torus of liquid around the periphery of the cup.

will be practically equal to the mean radial velocity $v_{\xi(m)}$ at the periphery as given by Equation 4-20, and (b) a tangential-velocity component 1/2(ωD). The liquid particles generally follow a straight path, and collide against the free surface of the liquid torus with a velocity v_h, which in the case of a nonviscous liquid will be equal to the total absolute velocity of the particle just beyond the periphery of the cup. The impact forces on the farthermost points of the torus are determined by the radial component $v_r(h)$.

Simple geometry shows that (for a nonviscous liquid):

$$v_r(h)^2 = \frac{\omega^2 D^2}{4}\left[1 - \frac{D^2}{(D + 2h)^2}\right] + v_D^2 \qquad (4\text{-}26)$$

or because, generally, $h \ll D$

$$v_r(h)^2 \approx \omega^2 Dh + v_D^2 \qquad (4\text{-}27)$$

The following simplifying assumptions have been made:

a) The radius of curvature at the farthermost point of the torus is approximately equal to $1/2(\delta_t)$.

b) The effect of the radius of curvature $1/2(D + 2h)$, is great with respect to $1/2(\delta_t)$.

c) The length h is proportional to δ_t, with the factor of proportionality being independent of the quantity Q, the viscosity μ, and the angular speed ω.

d) In Equation 4-27 the term v_D^2 may be neglected with respect to the term $\omega^2 Dh$; this is justified because generally v_D is small compared with $\omega(Dh)^{1/2}$.

e) The effect of viscosity on $v_r(h)$ will be accounted for by a simple power law of the Reynolds number $\rho v_r(h)\delta_t/\mu$.

Consequently,

$$v_r(h)^2 \propto \omega^2 D\delta_t \left(\frac{\rho v_r(h)\delta_t}{\mu}\right)^n \tag{4-28}$$

The condition for equilibrium between the impact forces and surface-tension forces at the farthermost points of the liquid torus yields

$$\rho v_r(h)^2 \propto \frac{\sigma}{\delta_t} \tag{4-29}$$

From Equations 4-28 and 4-29, the value of δ_t can be obtained,

$$\frac{\delta_t}{D} \propto \left(\frac{\sigma}{\rho\omega^2 D^3}\right)^{\frac{2}{4+n}} \left(\frac{\mu^2}{\rho\sigma D}\right)^{\frac{n}{4+n}} \tag{4-30}$$

In order to determine the number of ligaments z, a simplified calculation is used. Seeing that, generally, $\delta_t/D \ll 1$, and that the cross section of the torus is approximately circular, one might tend to consider the torus as a straight column of liquid and to apply Rayleigh instability theory. However, instability of such a column, by the effect of surface tension alone, exists only in the case of disturbances of rotational symmetry. Because disturbances of rotational symmetry cannot occur on the liquid torus considered, Rayleigh's theory does not

apply. To account for non-symmetric disturbances, the following approximate calculation for a nonviscous liquid is presented.

First, assume a disturbance on the free surface of the torus of the following form:

$$\zeta = \zeta_0 e^{\beta t} \cos \frac{2\pi x}{\lambda} \cos n\theta \tag{4-31}$$

Consider the pressures acting at the farthermost points of the torus (that is, for $\theta = 0$).

The impact forces cause an excess pressure equal to $(1/2)(\rho\omega^2 D\zeta)$. The excess internal pressure to accelerate the liquid may be given by

$$-c\,\delta_t \rho \frac{\partial^2 \zeta}{\partial t^2} \tag{4-32}$$

where c is a constant. The surface tension causes an excess pressure

$$\sigma\left(\frac{4}{\delta_t^2} + \frac{4}{\delta_t^2}\frac{\partial^2}{\partial\theta^2} + \frac{\partial^2}{\partial x^2}\right)\zeta \tag{4-33}$$

The equilibrium condition at the free surface between these pressures then gives

$$c\,\delta_t \rho \frac{\partial^2 \zeta}{\partial t^2} - \frac{1}{2}\rho\omega^2 D\zeta - \sigma\left(\frac{4}{\delta_t^2} + \frac{4}{\delta_t^2}\frac{\partial^2}{\partial\theta^2} + \frac{\partial^2}{\partial x^2}\right)\zeta = 0 \tag{4-34}$$

Substitution of Equation 4-31 into Equation 4-34 yields

$$c\,\delta_t \rho \beta^2 - \frac{1}{2}\rho\omega^2 D - \frac{4\sigma}{\delta_t^2}\left(1 - s^2 - \frac{\pi^2\delta_t^2}{\lambda^2}\right) = 0 \tag{4-35}$$

The disturbance increases if β has a positive value, that is, if

$$\frac{\pi^2\delta_t^2}{\lambda^2} < \frac{\rho\omega^2 D\delta_t^2}{8\sigma} + 1 - s^2 \tag{4-36}$$

If all the bulges of the disturbance grow into ligaments, the relation between the number of ligaments z and the wavelength λ is

$$z = \pi D/\lambda \tag{4-37}$$

The right-hand term of the inequality (Equation 4-36) has approximately a constant value because δ_t is approximately inversely proportional

to ω; this suggests assuming a constant value for λ/δ_t. The maximum number of bulges will then be proportional to D/δ_t.

If the shape of the torus between two adjacent ligaments is visualized (see, for instance, Figure 4.11), it is apparent that the maximum number of ligaments cannot be equal to the maximum number of bulges, but must have a smaller value. If it is still assumed that the minimum possible spacing for the ligaments is proportional to δ_t, so that $z = D/\delta_t$ one obtains

$$z = \left(\frac{\rho\omega^2 D^3}{\sigma}\right)^{\frac{2}{4+n}} \left(\frac{\rho\sigma D}{\mu^2}\right)^{\frac{n}{4+n}} \tag{4-38}$$

In this expression, the parameter n has to be determined by experiment [8]. The results of previous experiments have yielded a value of $n = 4/5$.

The semi-empirical relation (Equation 4-38) with $n = 4/5$ is

$$z = 0.215\left(\frac{\rho\omega^2 D^3}{\sigma}\right)^{5/12} \left(\frac{\rho\sigma D}{\mu^2}\right)^{1/6} \tag{4-39}$$

This relation is used to calculate the number of teeth necessary to maintain ligament droplet formation and avoid sheet atomization when using a rotary device with teeth placed along the outer rim. The results are illustrated in Section 4.2.4.

The previous analysis has been concerned with ligament formation; however, liquid atomization--a result of the disintegration process--may be different for the three different states of disintegration. In the state of direct formation of droplets, the droplets are formed singly from protuberances originating from the bulges of the deformed liquid torus around the edge of the cup. The moment the droplets are split off from these protuberances generally will be different for the various droplets; this means that the protuberances will have different thicknesses and heights at the moment of droplet formation. Consequently, the various droplets will not have the same size; it is likely, however, that they will have diameters roughly the thickness of the liquid torus.

Equation 4-30 may then serve as a rough estimate of the mean drop size. The attachment of teeth on the periphery will constrain the protuberance thickness and height to be more uniform. This in turn should improve drop size uniformity.

In the state of ligament formation, the ligaments break up into droplets by disturbances of rotational symmetry. This process of breaking up, identical with that of a straight liquid column and agreeing with Rayleigh's instability theory, is clearly shown in Figure 4.11, page 60.

If all the ligaments have the same diameter, i.e., if they all break up at the same distance from the periphery of the cup and this occurs by disturbances of the optimum wavelength for rapid breakup, and if there is no effect of ligament stretching all droplets formed will have the same diameter. Without induced instabilities, however, the drops are not likely to be all the same size, and under actual conditions not all ligaments break up at the same distance from the periphery of the cup, so that the diameter of the ligaments at the breakup location is unequal for various ligaments. Breakup can also occur by singular disturbances at other than the optimum wavelength. Figure 4.11 shows a few cases of breakup by such singular disturbances. Stretching of the ligaments causes bigger drops to form with a thin thread of liquid trailing behind. This thin thread of liquid breaks up into very small droplets.

Nevertheless, the atomization is still more uniform if compared with results obtained with other methods of disintegration. The installation of teeth on the periphery will constrain both ligament size and breakup distance further improving drop size uniformity.

In the state of film formation, disturbing forces deform the film, and surface-tension action causes disruption of the film into many irregular ligaments and droplets, the latter are interconnected by thin threads of liquid which break up into fine droplets. It is reasonable to expect a less uniform atomization than that occurring in ligament formation. Because this nonuniformity is mainly caused by a greater

number of drops of very small size, the difference between both atomizations will be more pronounced if distribution curves by number are compared. One will need to regulate flow rate and velocity to eliminate the deleterious effects of sheet formation.

4.2.4 Dispersal Method and Conceptual Design--Rotating Device

In this type of device a number of teeth would be placed on the outside periphery of an instrument such as that schematically illustrated in Section 4.2.1. Grooved sides at position A (see Figure 4.9) will help to guide and regulate the flow as it is centrifugally forced to the outside. The number of teeth needed depends on the fluid characteristics, generator size, and rotational velocity. Table 4.1 illustrates the number of teeth needed as calculated from Equation 4-39. The number of teeth per centimeter is not overly prohibitive in any case. It will probably be helpful to lower the surface tension of the liquid thus enhancing the uniform flow of the liquid in the grooves. As mentioned, once the liquid reaches the teeth three types of droplet production can occur; direct droplet formation from the teeth (see Figure 4.15), ligament formation, with subsequent droplet formation, and sheet formation followed by irregular-sized droplet formation. The type of formation realized

TABLE 4.1. NUMBER OF TEETH REQUIRED TO MAINTAIN LIGAMENT FORMATION AS A FUNCTION OF ROTATIONAL VELOCITY AND DISK DIAMETER.

Diameter (cm)	Rotational Velocity (rpm)	Number of Teeth (cm)	Number of Teeth (per cm)
5	1000	37.6	2.4
5	3000	94.6	6.0
5	5000	145.4	9.3
10	1000	56.6	1.8
10	3000	142.5	4.5
10	5000	219.0	7.0
20	1000	85.2	1.4
30	3000	214.5	3.4
20	5000	330.0	5.2

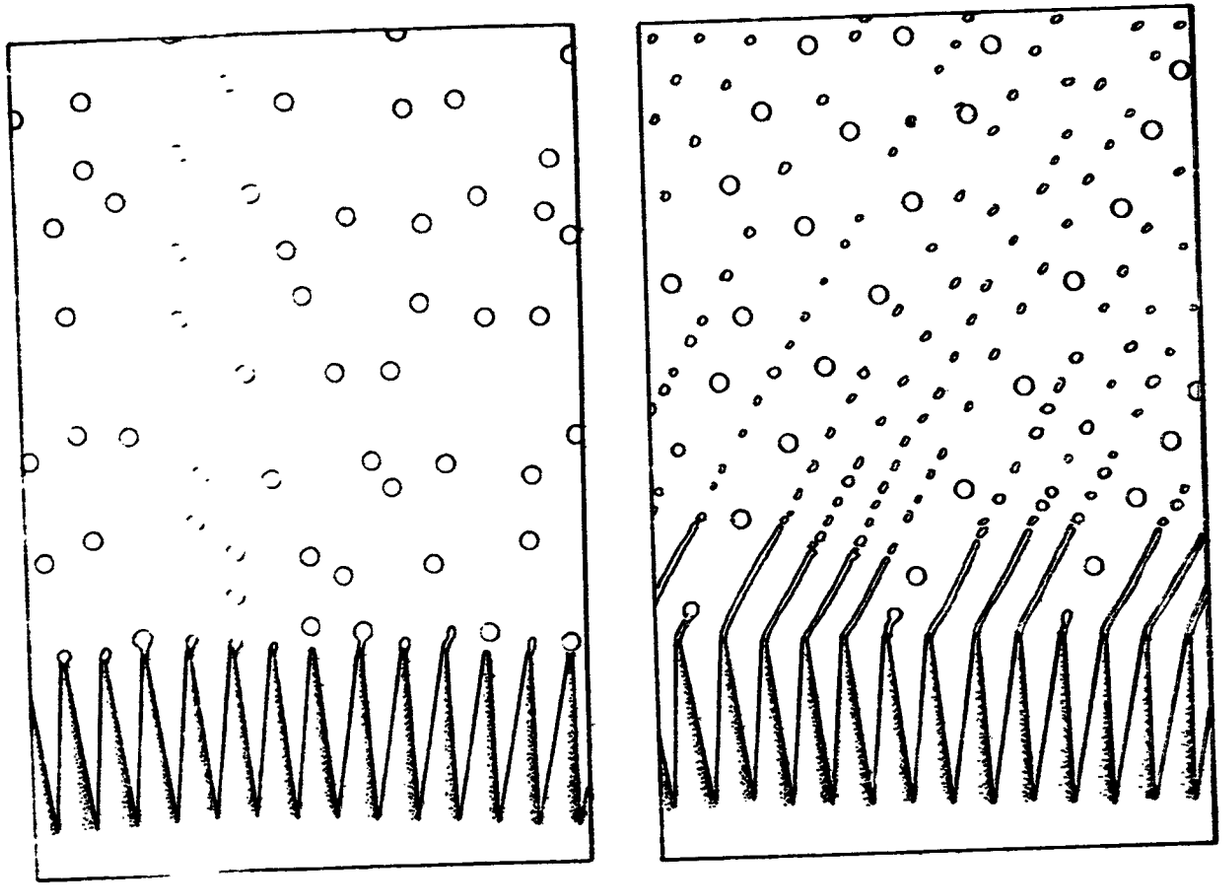

(a) Direct formation.

(b) Direct and ligament formation.

Figure 4.15 Illustration of rotary atomization, using a toothed rim.

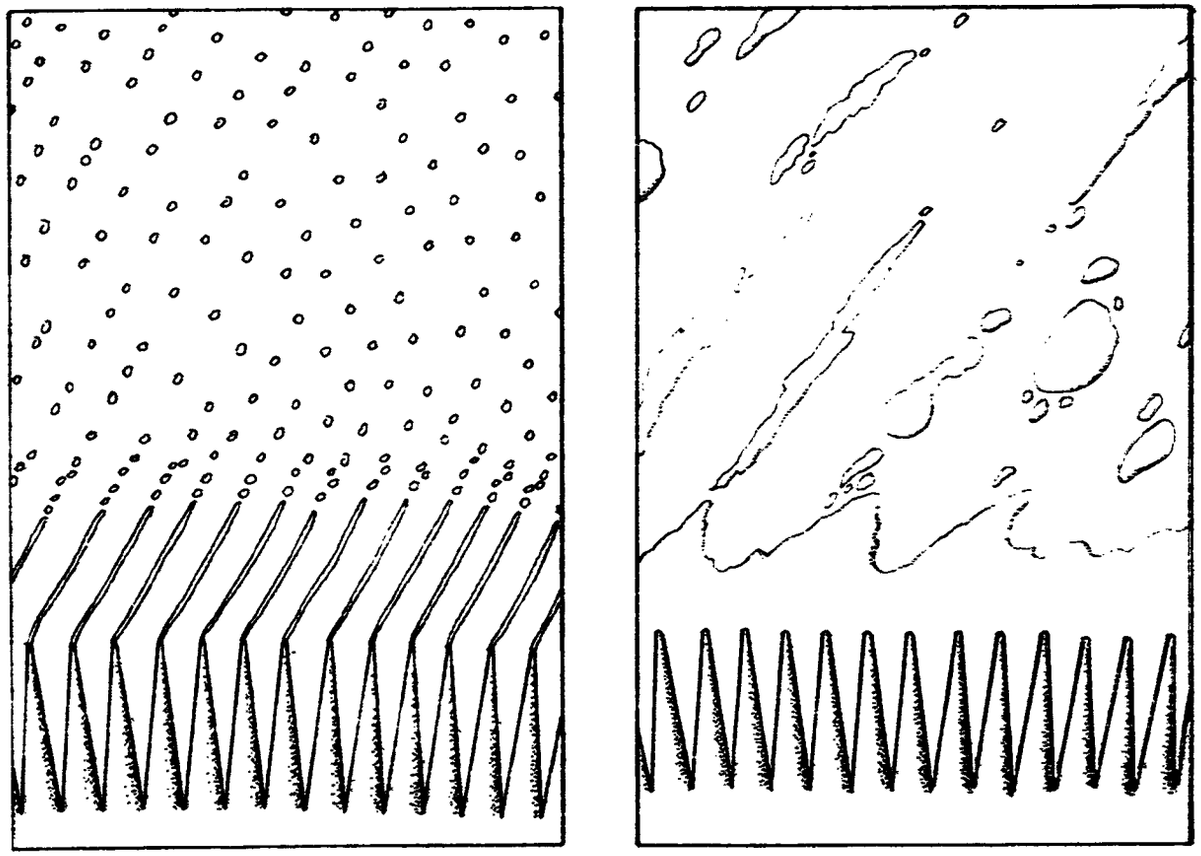

(c) Ligament formation.

(d) Sheet formation.

Figure 4.15 (continued)

depends on such parameters as viscosity, surface tension, liquid feed rate, etc. To obtain "monodisperse" droplets one needs to maintain either direct formation or ligament formation. This can be achieved by varying the parameters involved. In order to obtain the coverage rates required for agricultural applications the devices could be rotated using small electric motors or airfoils designed to maintain particular rotational rates at certain airspeeds. The system then will consist of a grooved half cone, or multiple units, with teeth on the periphery, driven by a small electric motor or appropriately designed airfoil with liquid being fed to the inside and centrifugally forced to the tips of the teeth. A diagram illustrating one possible setup is presented in Figure 4.16. The system should be a great improvement over present conventional hydraulic or air atomizing nozzles. Detailed engineering drawings and analyses should be developed in the next phase of this endeavor.

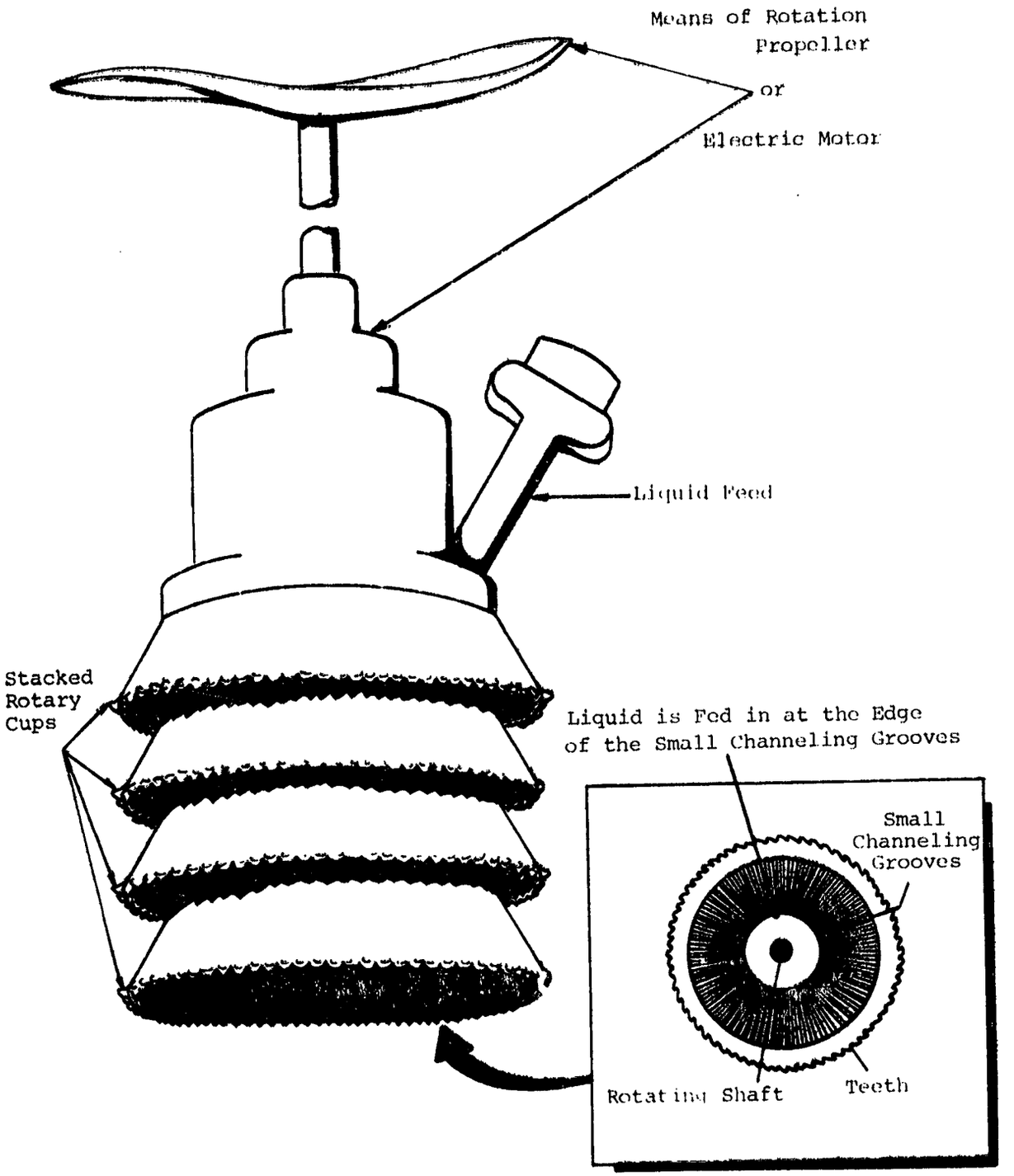

Figure 4.16 Diagram illustrating rotary atomization concept.

5.0 CONCLUDING REMARKS

After a survey of the literature concerned with spray atomization, two conceptual ideas to produce "monodisperse" droplets for agricultural applications have been conceived. The two ideas are such that the range of common characteristics of agricultural chemicals such as surface tension, viscosity, and density do not render the two techniques impractical for producing "monodisperse" droplets for agricultural applications. Both techniques will be capable of producing sufficient numbers of droplets to give adequate foliage coverage when using concentrated solutions. Some modifications will be needed if dilute solutions are to be effectively dispersed. Both techniques use the basic principle of Rayleigh instability to form the droplets. The two ideas can be described as a vibrating orifice and a rotating disk with appropriately spaced teeth along the periphery. The two devices will not require elaborate electronics or fluid systems and changes in drop size can be made easily. The drop size, when using different chemicals with different chemical characteristics, can be maintained by varying the vibration frequency or the peripheral speed. Only under extreme conditions will it be necessary to change nozzles. If, however, a nozzle change is necessary, the nozzles can be designed so that exchanging them can be done both quickly and easily.

The production of copious quantities of small droplets (20 μm diameter) will, however, probably require special modifications. For example, utilizing the vibrating orifice device for production of very small droplets will require adequate filtering to insure non-clogging of the orifices. The number of droplets can be increased by increasing the number of orifices. Practicality of the system will decrease as the droplet size decreases.

When using a rotating disk to produce small droplets, it will probably be necessary to use a spray tube (device to eliminate larger droplets and recycle the fluid). The spray tubes could successfully

eliminate droplets larger than the desired sizes. By placing rotary-type atomizers within a spray tube with a suitable diameter, the droplet spectrum emitted can be effectively controlled. Considerable savings in spray material can also be realized. Droplets of 25 μm volume mean diameter will be more difficult to produce than the larger sizes but it is felt the technique, with slight modifications, will be able to effectively produce such small droplets.

After dispersal the drop distribution can be significantly changed by parameters such as turbulence and shear. Both shearing of larger drops and coalescence of all drop sizes may occur. The very reasons for producing "monodisperse" droplets, i.e., better plant coverage, less drift, and more effective use of pesticides would be frustrated if the drop size impacting on the target were polydisperse due to coalescence and shearing effects. One needs not only produce monodisperse droplets but develop methods for maintaining that monodispersity until the chemicals reach the target. Preliminary ideas such as charging the chemicals look promising in this regard but further research is needed before definite conclusions can be drawn.

Proper engineering of the two conceptual ideas presented should result in two good methods for production of monodisperse droplets for agricultural applications. The cost to benefit ratio of such a production method is extremely good and further research should be carried out if at all possible.

6.0 REFERENCES

1. Lane, W. R. Journal of Scientific Instruments, Vol. 24, pp. 68, 1947.

2. Reil, K., and J. Hallett. "An Apparatus for the Production of Uniform Sized Water Drops, at Desired Time Intervals," The Review of Scientific Instruments, Vol. 40, No. 4, pp. 533-534, 1969.

3. Blanchard, D. C. "A Simple Method for the Production of Homogeneous Water Drops Down to 1 Micron Radius," Journal of Colloid Science, Vol. 9, pp. 321-328, 1954.

4. Mason, B. J., O. W. Jayaratne, and J. D. Woods. "An Improved Vibrating Capillary Device for Producing Uniform Water Droplets of 15 to 500 Micron Radius," Journal of Scientific Instruments, Vol. 40, pp. 247-249, 1963.

5. Mercer, T. T., R. F. Goddard, and R. L. Flores. "Output Characteristics of Three Ultrasonic Nebulizers," Annals of Allergy, Vol. 26, pp. 18-27, 1968.

6. Lang, R. J. "Ultrasonic Atomization of Liquids," Journal of the Acoustic Society of America, Vol. 34, No. 6, 1962.

7. Gauthier, W. D. "Operational Characteristics of the Ultrasonic Nebulizer," Proceedings of the First Conference on Clinical Applications of the Ultrasonic Nebulizer, Chicago, Illinois, 1966.

8. Hinze, J. O., and H. Milborn. "Atomization of Liquids by Means of a Rotating Cup," Journal of Applied Mechanics, Vol. 17, pp. 145-153, June 1950.

9. Ranz, W. E. Chemical Engineering Progress, Vol. 48, p. 247, 1952.

10. Adler, C. R., and W. R. Marshall. Chemical Engineering Progress, Vol. 47, pp. 515-601, 1951.

11. Herring, W. M., and W. R. Marshall. Paper presented at the American Industrial Chemical Engineers meeting in St. Lousi, Missouri, 1953.

12. Johnstone, K. A., and D. R. Johnstone. "Power Requirements and Droplet Size Characteristics of a New Ultra-Low-Volume, Hand-Carried, Battery-Operated Insecticide Sprayer," Misc. Report 26, published by the Center for Overseas Pest Research, College House, Wrights Lane, London W8 5SJ, United Kingdom.

13. Savert, F. Annals of Chemistry, Vol. 53, p. 337 (1883); Lord Rayleigh, "Theory of Sound," Vol. II, pp. 362-364, Dover, New York (1945).

14. Plateau. "Statique experimentale et theorique des liquides soumix aux sules forces molecularies," Rayleigh, Vol. II, pp. 360, 363, 364, Dover, New York, 1945.

15. Lord Rayleigh. London Mathematical Society, Proceedings, Vol. 10, p. 7 (1878); Lord Rayleigh, "Theory of Sound," Vol. II, pp. 361-365, Dover, New York (1945).

16 ber, C., and Z. Agnew. Mathematical Mechanics, Vol. 11, p. 136, 231.

17. Fraser, R. P., P. Eisenklam, N. Dombrowski, and D. Hasson. American Industrial Chemical Engineers Journal, Vol. 8, p. 672, 1962.

18. Miesse, C. C. Industrial Engineering Chemistry, Vol. 47, p. 1690, 1965.

19. Grant, R. P., and S. Middleman. American Industrial Chemical Engineers Journal, Vol. 12, No. 4, pp. 669-678, 1966.

20. Akesson, N. B., W. E. Yates, and R. E. Cowden. "Procedures for Evaluating the Potential Losses during the Following Pesticide Application," 1977 Winter Meeting of the American Society of Agricultural Engineers, Paper No. 77-1504.

21. Butler, B. J., N. B. Akesson, and W. E. Yates. "Use of Spray Adjuvants to Reduce Drift," Transactions of the American Society of Agricultural Engineers, Vol. 12, No. 2, pp. 182-186, 1969.

22. Lord Rayleigh. London Mathematical Society, Proceedings, Vol. 10, No. 4, 1878.

23. Bogy, D. B. "Use of One-Dimensional Cosserat Theory to Study Instability in a Viscous Liquid Jet," Physics of Fluids, Vol. 21, No. 2, pp. 190-197, February 1978.

24. Green, A. E. International Journal of Engineering Science, Vol. 14, No. 49, 1976.

25. Pimbley, W. T. IBM Journal of Research and Development, Vol. 20, No. 148, 1976.

26. Lee, H. C. IBM Journal of Research and Development, Vol. 18, No. 64, 1974.

27. Weber, C., and Z. Agnew. Mathematical Mechanics, Vol. 11, No. 136, 1931.

28. Bouse, L. F. "Experimental Study of the Use of Pulsed Jets to Atomize Various Liquids," Transactions of the American Society of Agricultural Engineers, Vol. 18, No. 4, pp. 618-622.

1. Report No.	2. Government Accession No.	3. Recipient's Catalog No.
NASA CR-159777		

4. Title and Subtitle	5. Report Date
MONODISPERSE ATOMIZERS FOR AGRICULTURAL AVIATION APPLICATIONS	February 1980
	6. Performing Organization Code
7. Author(s)	8. Performing Organization Report No
Larry S. Christensen and Sidney L. Steely	None
	10. Work Unit No.
9. Performing Organization Name and Address	11. Contract or Grant No
FWG Associates, Inc. R.R. 2, Box 271-A Tullahoma, Tennessee 37388	NAS3-21582
	13. Type of Report and Period Covered
12. Sponsoring Agency Name and Address	Contractor Report
National Aeronautics and Space Administration Washington, D.C. 20546	14 Sponsoring Agency Code

15. Supplementary Notes

Final report. Project Manager, Robert Ingebo, Airbreathing Engines Division, NASA Lewis Research Center, Cleveland, Ohio 44135.

16. Abstract

Based on the information obtained from a literature survey of atomization techniques and agricultural aviation spray applications, two monodisperse spray nozzles were conceived and the rationale used in each conceptual nozzle design documented. The work was undertaken to eliminate present problems in agricultural aviation applications, such as ineffective plant coverage, drift due to small droplets present in spray being dispersed, and nonuniform swath coverage. Presently, treatment effectiveness is limited due to polydisperse droplet distributions being sprayed. The production of monodisperse droplet distributions can greatly improve application pest mortality, swath coverage, drift reduction, and decrease potential environmental pollution. Monodisperse droplet production will also ultimately help to optimize total crop output while minimizing deleterious effects on the environment.

17. Key Words (Suggested by Author(s))	18. Distribution Statement
Liquid atomization Monodisperse sprays Agricultural aviation	Unclassified - unlimited STAR Category 34

19. Security Classif. (of this report)	20. Security Classif. (of this page)	21. No. of Pages	22. Price*
Unclassified	Unclassified	80	

* For sale by the National Technical Information Service, Springfield Virginia 22161

98